SIAM J. APPL. MATH.
Vol. 80, No. 5, pp. 2144–2169

HOW DOES DISPERSAL AFFECT THE INFECTION SIZE?*

DAOZHOU GAO†

Dedicated to Professor Jifa Jiang on his 65th birthday

Abstract. Human movement facilitates the spatial spread of infectious diseases and poses a serious threat to disease prevention and control. A large number of spatial epidemic models have been proposed and analyzed in the past few decades. The vast majority of these studies focus on establishing a threshold result between disease persistence and extinction in terms of the basic reproduction number. In reality, disease eradication is difficult and even impossible for many infectious diseases. Thus, it is crucial to understand how population dispersal affects the total infection size and its distribution across the environment. Based on a susceptible-infected-susceptible patch model with standard incidence, some general results on the number of infections over all patches and disease prevalence in each patch are obtained. For the two-patch submodel, we give a complete classification of the model parameter space as to whether dispersal is beneficial or detrimental to disease control. Particularly, fast diffusion decreases the basic reproduction number but may increase the total infection size, highlighting the necessity of evaluating control measures with other quantities besides the basic reproduction number. Higher infection risk means higher disease prevalence in the two-patch case. However, numerical simulations find that the patch with the highest risk of infection may not have the highest disease prevalence when three or more patches are concerned. Besides spatial heterogeneity and diffusion coefficient, the total infection size is also significantly affected by patch connectivity.

Key words. human movement, infection size, disease prevalence, basic reproduction number, diffusion coefficient, endemic equilibrium

AMS subject classifications. 92D30, 91D25, 34C60, 34D05, 37N25

DOI. 10.1137/19M130652X

1. Introduction.

Human migration and tourism play an important role in the spatial spread of infectious diseases. On the one hand, infected humans reach disease-free regions, transmit infectious agents to local residents, and incur disease outbreaks. This process happens repeatedly over time, e.g., 2003 SARS outbreak [33], 2009 H1N1 influenza pandemic [27], 2015–2016 Zika virus disease epidemic [45], and 2019–2020 coronavirus disease pandemic [46]. On the other hand, imported cases pose a big challenge to nonendemic countries in achieving or maintaining elimination status. About 1,700 malaria cases are reported annually in the United States even though the disease was eliminated from the country in the early 1950s [32]. With transportation and economic development, different regions have stronger connection and humans travel more frequently than ever before. However, during severe disease outbreaks like the ongoing COVID-19 outbreak, flight cancellations, border closures, and travel restrictions are implemented in many countries and regions, which dramatically reduce human mobility. These changes urge public agencies to pay increasing attention to investigate the effects of travel on the geographical spread of infectious diseases.

*Received by the editors December 13, 2019; accepted for publication (in revised form) June 9, 2020; published electronically September 22, 2020.
https://doi.org/10.1137/19M130652X
Funding: This work was supported by the National Natural Science Foundation of China (12071300), the Natural Science Foundation of Shanghai (20ZR1440600), Program for Professor of Special Appointment (Eastern Scholar) at Shanghai Institutions of Higher Learning (TP2015050), and Shanghai Gaofeng Project for University Academic Development Program.
†Department of Mathematics, Shanghai Normal University, Shanghai 200234, People's Republic of China (dzgao@shnu.edu.cn).

Many compartmental models consisting of multiple patches (countries, cities, communities, etc.) have been developed to study the spread of general or specific diseases in discrete space [5, 41]. Wang and coauthors [26, 40, 42, 43] studied the dynamics of SIS patch models with bilinear incidence and standard incidence. Salmani and van den Driessche [34] proposed an SEIRS patch model by incorporating incubation period and temporary immunity. Cui, Takeuchi, and Saito [10] formulated a two-patch SIS model that includes infection during transport. Liu and Takeuchi [30] further considered the joint effect of transport-related infection and entry-exit screening through a two-patch SIQS model. Sun et al. [36] and Gao and Ruan [20] analyzed an SIS model with the consideration of behavior change to describe disease spread between two patches and an arbitrary number of patches, respectively. Arino and Portet [6] modeled the disease spread between a large urban center and some smaller neighboring satellite cities via an SIR infectious disease propagation model where the urban center has standard incidence and the satellite cities have bilinear incidence. Cosner et al. [9] presented two classes of the multipatch Ross–Macdonald model to explore how human movement affects vector-borne disease transmission. Gao and Ruan [21] introduced a more detailed multipatch malaria model with SEIRS structure for humans and SEI structure for mosquitoes.

So far most existing theoretical works concentrate on analyzing the dynamical behavior of model systems. Threshold results can usually be established in terms of the basic reproduction number $\mathcal{R}_0$. Namely, if $\mathcal{R}_0 < 1$, then the disease dies out, while if $\mathcal{R}_0 > 1$, then the disease is uniformly persistent in all patches. The multipatch reproduction number is determined by spatial heterogeneity, habitat connectivity, and movement rates [1]. For the simple SIS patch model with standard incidence, the multipatch reproduction number is bounded below and above by the minimum and maximum values of the patch reproduction numbers [20], which means that the disease becomes persistent or extinct in all connected patches if the disease spreads or disappears in each isolated patch. However, for the SIS patch model with bilinear incidence [43] or the multipatch Ross–Macdonald model [9], population dispersal may induce disease spread even though the disease dies out in each isolated patch. Gao and Ruan [21] numerically found that human movement can drive malaria to persist or die out even if the disease goes extinct or persistent in two disconnected but identical patches. Moreover, nonhomogeneous mixing between hosts and vectors alone can result in a larger basic reproduction number for both visitation model and migration model [22, 23]. In brief, population dispersal may intensify or weaken the persistence of infectious diseases.

When an infectious disease becomes endemic in a patchy environment, a natural question is how human movement affects the infection size or disease prevalence (i.e., the proportion of individuals in a population having a specific disease or a particular condition) across the environment. In particular, we are interested in finding the conditions under which dispersal results in more infections than nondispersal. As we know, the basic reproduction number measures the initial transmission potential, but can rarely characterize the endemic level of the infection. For the classical Ross–Macdonald model, Dye and Hasibeder [13] showed that the number of host infections initially increases then decreases with host size, whereas $\mathcal{R}_0$ is strictly decreasing in host size. Few studies on examining the influence of human movement on infection size or disease prevalence over all patches are available. Hsieh, van den Driessche, and Wang [25] developed an SEIRP multipatch model with partial immunity and presented a numerical example in which banning travel of sick individuals from the high to the low prevalence patch can have a negative impact on the overall disease prevalence.

Based on a multipatch Ross–Macdonald model without spatial heterogeneity, Gao, van den Driessche, and Cosner [22] found that the difference of the overall prevalence in humans with and without dispersal may be constantly positive or change sign when the diffusion rates of humans and mosquitoes vary. For a two-group multipatch SIS model, Gao [17] demonstrated that infrequent travelers in the high risk patch (where the patch reproduction number is larger) and the low risk patch (where the patch reproduction number is smaller), respectively, have the highest and the lowest disease prevalence. However, there is yet no systematic work towards answering the aforementioned question. The main difficulty lies in the facts that the uniqueness and global attractivity of the endemic equilibrium are generally unknown and the explicit expression of the total number of infections at the endemic equilibrium is unavailable or intractable.

It is worth noting that a pretty similar question in ecology is how the population size and distribution of animals change with dispersal [11]. The maximal total population abundance is desirable for an endangered species, while we seek to minimize the abundance of an insect pest. Freedman and Waltman [15] analyzed a two-patch logistic model and proved that sufficiently high dispersal increases the total population abundance if there is a positive relationship between intrinsic growth rate and local carrying capacity. Holt [24] generalized these results to a source-sink system. Recently, Arditi, Lobry, and Sari [3, 4] gave a full mathematical analysis of the model of Freedman and Waltman [15] with symmetric and asymmetric dispersal. Wang [44] studied the effect of dispersal on the total pollinator abundance according to a two-patch pollination-mutualism model where only the pollinator can move between patches. Lou [31] observed that continuous diffusion in a heterogeneous environment increases the total population size if the intrinsic growth rate is proportional to carrying capacity. Zhang et al. [47] proposed a consumer-resource model in a continuous spatial setting and tested it mathematically and experimentally. The reader may refer to DeAngelis, Ni, and Zhang [11] for more references on the effects of diffusion on the total biomass in discrete and continuous space. Although the method and theory in ecology could inspire the study in epidemiology, we can expect that the latter is possibly more challenging since only the infected subpopulation instead of the whole population is concerned.

The main aim of this paper is to study the effect of population dispersal on total infection size. In the next section, we formulate an SIS patch model with standard incidence and present some preliminaries. In section 3, the asymptotic values of the total infection size at the endemic equilibrium as the diffusion rate goes to zero and infinity, respectively, are derived and compared. The disease prevalence of each patch is estimated. Section 4 is devoted to a detailed study of the two-patch case. Numerical examples are given to further explore the effect of population dispersal on the local and global disease prevalence in section 5. The paper ends with a brief discussion.

2. The model. We consider an environment consisting of n patches connected by human migration. The total population in patch $i \in \Omega = \{1, \dots, n\}$, denoted by N_i, is divided into the susceptible and infected classes, with S_i and I_i denoting the respective numbers. Allen et al. [1] studied the following SIS patch model:

$$\begin{aligned} \frac{dS_i}{dt} &= -\beta_i \frac{S_i I_i}{N_i} + \gamma_i I_i + \delta \sum_{j \in \Omega} L_{ij} S_j, \ i \in \Omega, \\ \frac{dI_i}{dt} &= \beta_i \frac{S_i I_i}{N_i} - \gamma_i I_i + \varepsilon \sum_{j \in \Omega} L_{ij} I_j, \ i \in \Omega, \end{aligned} \tag{2.1}$$

where β_i and γ_i are positive transmission and recovery rates, respectively; L_{ij} is the degree of incoming movement from patch j to patch i for $i \neq j$, and $-L_{ii} = \sum_{j \neq i} L_{ji}$ is the degree of outgoing movement from patch i to all other patches; and δ and ε are positive diffusion coefficients of the susceptible and infected subpopulations, respectively.

Assume that the connectivity matrix $L = (L_{ij})$ is irreducible. Then the model (2.1) has a unique disease-free equilibrium $E_0 = (\boldsymbol{N}^*, \boldsymbol{0})$, where $\boldsymbol{N}^* = (N_1^*, \ldots, N_n^*)$ is the unique positive solution of

$$\sum_{j \in \Omega} L_{ij} N_j = 0,\ i \in \Omega, \quad \text{and} \quad \sum_{i \in \Omega} N_i = \sum_{i \in \Omega} (S_i(0) + I_i(0)) := N > 0.$$

More precisely, it follows from Lemma 3.1 in Gao and Dong [18] that

$$(N_1^*, \ldots, N_n^*) = \frac{N}{\sum_{i \in \Omega} L_{ii}^*} (L_{11}^*, \ldots, L_{nn}^*), \tag{2.2}$$

where L_{ii}^* is the (i,i)-cofactor of L and $\operatorname{sgn}(L_{ii}^*) = (-1)^{n-1}$. In particular, if L is symmetric or line-sum-symmetric (i.e., the ith row sum of L equals the ith column sum of L for all $i \in \Omega$), then $L_{11}^* = \cdots = L_{nn}^*$ and hence $N_1^* = \cdots = N_n^* = N/n$.

The new infection and transition matrices of model (2.1) are, respectively,

$$F = \operatorname{diag}\{\beta_1, \ldots, \beta_n\} \quad \text{and} \quad V = \operatorname{diag}\{\gamma_1, \ldots, \gamma_n\} - \varepsilon L.$$

Thus, by the next generation matrix method [12, 39], the basic reproduction number of model (2.1) is defined as

$$\mathcal{R}_0 = \rho(FV^{-1}).$$

Obviously, the basic reproduction number of patch i in isolation is $\mathcal{R}_0^{(i)} = \beta_i/\gamma_i$. Allen et al. [1] showed that the disease-free equilibrium E_0 is globally asymptotically stable if $\mathcal{R}_0 < 1$, and there exists a unique endemic equilibrium E^* if $\mathcal{R}_0 > 1$ and L is symmetric. Two main theorems relate spatial heterogeneity, habitat connectivity, and movement rates to disease persistence and extinction. They left three open problems concerning the monotonicity of $\mathcal{R}_0$ with respect to ε, the global attractivity of E^*, and the asymptotic behavior of E^* as $\delta \to 0$, respectively. The first problem was recently answered by Gao [17] and Gao and Dong [18], while some progress in solving the remaining two problems was made by Li and Peng [28] and Chen et al. [8]. To facilitate the study of the impact of human movement on the total number of infections, we make the following assumptions throughout the paper:

(B1) $S_i(0) \geq 0$ and $I_i(0) > 0$ for $i \in \Omega$.
(B2) L is essentially nonnegative and irreducible.
(B3) $\mathcal{R}_0^{(i)}$ is nonconstant in $i \in \Omega$.
(B4) The population distribution by patch obeys (2.2) as $\delta = \varepsilon = 0$ (no dispersal).
(B5) The diffusion coefficients of the susceptible and infected subpopulations are the same.

The first two assumptions mean that the disease initially presents in every patch and the n patches cannot be separated into disconnected parts, respectively. If (B3) fails, then Proposition 2.2 in Gao and Ruan [20] implies that $\mathcal{R}_0$ is constant for any ε and L. Meanwhile, the total number of infections at the endemic equilibrium equals $\max\{(1 - 1/\mathcal{R}_0)N, 0\}$, which is also independent of ε and L. The fourth assumption guarantees that the population size of each patch in isolation is the same as that of

the patch in connection with $\delta = \varepsilon \to 0+$ or at the disease-free equilibrium. The last assumption is acceptable when a disease like the common cold has a mild effect on the mobility of infected people. It enables us to establish the global asymptotic stability of the endemic equilibrium. In fact, if $\delta = \varepsilon$, then model (2.1) becomes

$$\begin{aligned} \frac{dS_i}{dt} &= -\beta_i \frac{S_i I_i}{N_i} + \gamma_i I_i + \varepsilon \sum_{j\in\Omega} L_{ij} S_j,\ i \in \Omega, \\ \frac{dI_i}{dt} &= \beta_i \frac{S_i I_i}{N_i} - \gamma_i I_i + \varepsilon \sum_{j\in\Omega} L_{ij} I_j,\ i \in \Omega. \end{aligned} \tag{2.3}$$

The total population in patch i obeys

$$\frac{dN_i}{dt} = \varepsilon \sum_{j\in\Omega} L_{ij} N_j,\ i \in \Omega, \quad \text{and} \quad \sum_{i\in\Omega} N_i = N > 0,$$

which has a globally asymptotically stable positive equilibrium $\boldsymbol{N}^* = (N_1^*, \dots, N_n^*)$ satisfying (2.2). Replacing N_i with N_i^* in the second equation of system (2.3) gives the limit system

$$\frac{dI_i}{dt} = \beta_i \left(1 - \frac{I_i}{N_i^*}\right) I_i - \gamma_i I_i + \varepsilon \sum_{j\in\Omega} L_{ij} I_j,\ i \in \Omega. \tag{2.4}$$

By the theory of monotone dynamical systems [35] and asymptotically autonomous systems [7], the global dynamics of system (2.3) are fully determined by the basic reproduction number.

THEOREM 2.1 (Corollary 3.5 in Gao and Ruan [20]). *For model* (2.3)*, the disease-free equilibrium E_0 is globally asymptotically stable in $\mathbb{R}_+^{2n}$ if $\mathcal{R}_0 \le 1$, and there exists a unique endemic equilibrium*

$$E^* = (\boldsymbol{S}^*, \boldsymbol{I}^*) = (S_1^*, \dots, S_n^*, I_1^*, \dots, I_n^*) = (N_1^* - I_1^*, \dots, N_n^* - I_n^*, I_1^*, \dots, I_n^*),$$

which is globally asymptotically stable on the nonnegative orthant minus the disease-free state if $\mathcal{R}_0 > 1$.

For system (2.4), if $\mathcal{R}_0 > 1$, then $(I_1^*, \dots, I_n^*)$ is the unique positive solution to

$$\beta_i \left(1 - \frac{I_i}{N_i^*}\right) I_i - \gamma_i I_i + \varepsilon \sum_{j\in\Omega} L_{ij} I_j = 0,\ i \in \Omega. \tag{2.5}$$

In what follows, we will investigate how human movement affects the total number of infections over all patches. In particular, when is it detrimental or beneficial to disease control in terms of infection size? Mathematically speaking, we will analyze the dependence of the total infection size at the positive stationary solution

$$T_n(\varepsilon) := \sum_{i\in\Omega} I_i^*(\varepsilon)$$

with respect to the diffusion coefficient $\varepsilon \ge 0$ and see when $T_n(\varepsilon)$ is greater or smaller than $T_n(0)$ (no dispersal). Note that system (2.4) can be viewed as a single species multipatch logistic model, which has been studied from the aspect of dynamical behavior and total biomass by many researchers [3, 4, 11, 14, 15, 21, 24, 37]. Nevertheless, in theoretical ecology, the matrix of connectivity is usually assumed to be symmetric and a sink patch does not have density-dependent mortality.

3. General results. First of all, we present a lemma on the basic reproduction number and the spectral bound of the Jacobian matrix of system (2.1) at the disease-free equilibrium with respect to the diffusion coefficient of the infected subpopulation, which ensures that if $T_n(\varepsilon_0) = 0$ for some $\varepsilon_0 \in [0,\infty)$, then $T_n(\varepsilon) \equiv 0$ for any $\varepsilon \in [\varepsilon_0,\infty)$. The interested reader may refer to a recent paper by Gao and Dong [18] for the proof and more details.

LEMMA 3.1. *For model* (2.1)*, the basic reproduction number* $\mathcal{R}_0(\varepsilon) = \rho(FV^{-1})$ *and the spectral bound* $s(\varepsilon) := s(F-V) = s(F-D+\varepsilon L)$ *are strictly decreasing and strictly convex in* $\varepsilon \in [0,\infty)$*, where* $D = \operatorname{diag}\{\gamma_1,\dots,\gamma_n\}$*. Moreover, we have*

$$\min_{i\in\Omega}\mathcal{R}_0^{(i)} < \mathcal{R}_0(\infty) = \sum_{i\in\Omega}\beta_i L_{ii}^* \Big/ \sum_{i\in\Omega}\gamma_i L_{ii}^* < \mathcal{R}_0(\varepsilon) < \mathcal{R}_0(0) = \max_{i\in\Omega}\mathcal{R}_0^{(i)},\ \forall \varepsilon > 0,$$

where $\mathcal{R}_0^{(i)} = \beta_i/\gamma_i$ *is nonconstant in* $i \in \Omega$ *and* L_{ii}^* *is the* (i,i)*-cofactor of* L*. In addition, if* $\mathcal{R}_0(0) > 1$*, then the following hold:*

(a) *If* $\mathcal{R}_0(\infty) < 1$*, then there exists a unique critical value* $\varepsilon^* \in (0,\infty)$ *such that* $\mathcal{R}_0(\varepsilon) > 1$ *for* $\varepsilon < \varepsilon^*$*,* $\mathcal{R}_0(\varepsilon) = 1$ *for* $\varepsilon = \varepsilon^*$*, and* $\mathcal{R}_0(\varepsilon) < 1$ *for* $\varepsilon > \varepsilon^*$*.*

(b) *If* $\mathcal{R}_0(\infty) \ge 1$*, then we have* $\mathcal{R}_0(\varepsilon) > 1$ *for all* $\varepsilon \ge 0$*.*

Remark 3.2. When $\mathcal{R}_0(0) > 1 > \mathcal{R}_0(\infty)$, the critical value ε^* exists and is actually the least positive root to the $(n-1)$th degree polynomial equation $\det(F-D+\varepsilon L) = 0$. For the two-patch case, a straightforward calculation yields

$$\varepsilon^* = \frac{(\beta_1-\gamma_1)(\beta_2-\gamma_2)}{(\beta_1-\gamma_1)L_{12} + (\beta_2-\gamma_2)L_{21}}.$$

When three patches are concerned, ε^* is a positive root of the quadratic equation

$$c_2\varepsilon^2 + c_1\varepsilon + c_0 = 0,$$

where

$$c_2 = \sum_{i=1}^{3}(\beta_i-\gamma_i)L_{ii}^* < 0,\quad c_1 = \sum_{i=1}^{3}\left(\prod_{j\ne i}(\beta_j-\gamma_j)\right)L_{ii},\quad \text{and } c_0 = \prod_{i=1}^{3}(\beta_i-\gamma_i).$$

Next we calculate the total number of infections at the stable steady state as $\varepsilon \to 0+$ and ∞. Denote the positive part of m by $m^+ = \max\{m,0\}$.

THEOREM 3.3. *For model* (2.3)*, we have*

$$T_n(0) = \sum_{i\in\Omega} I_i^*(0) = \sum_{i\in\Omega}\left(1-\frac{1}{\mathcal{R}_0^{(i)}}\right)^+ N_i^*$$

and

$$T_n(\infty) = \sum_{i\in\Omega} I_i^*(\infty) = \left(1-\frac{1}{\mathcal{R}_0(\infty)}\right)^+ N,$$

where

$$I_i^*(0) := \lim_{\varepsilon\to 0+} I_i^*(\varepsilon) = \left(1-\frac{1}{\mathcal{R}_0^{(i)}}\right)^+ N_i^*,\ i\in\Omega,$$

$$I_i^*(\infty) := \lim_{\varepsilon\to\infty} I_i^*(\varepsilon) = \left(1-\frac{1}{\mathcal{R}_0(\infty)}\right)^+ N_i^*,\ i\in\Omega.$$

Proof. If $\varepsilon \to 0+$, then the transmission dynamics of patch $i \in \Omega$ can be described by a single patch SIS model,

$$\frac{dS_i}{dt} = -\beta_i \frac{S_i I_i}{N_i^*} + \gamma_i I_i,$$
$$\frac{dI_i}{dt} = \beta_i \frac{S_i I_i}{N_i^*} - \gamma_i I_i,$$

where $S_i(t) + I_i(t) = N_i^*$. Thus,

$$I_i(t) \to \max\left\{(1 - 1/\mathcal{R}_0^{(i)})N_i^*, 0\right\} = (1 - 1/\mathcal{R}_0^{(i)})^+ N_i^* \quad \text{as} \quad t \to \infty.$$

Suppose $\mathcal{R}_0(\infty) \geq 1$. It follows from Theorem 3.6 in Gao and Dong [18] that

$$\lim_{\varepsilon \to \infty} (I_1^*(\varepsilon), \ldots, I_n^*(\varepsilon)) = m(|L_{11}^*|, \ldots, |L_{nn}^*|) = m(-1)^{n-1}(L_{11}^*, \ldots, L_{nn}^*)$$

for some $m \geq 0$. Summing up (2.5) over i from 1 to n gives

$$\sum_{i\in\Omega} \left(\beta_i \left(1 - \frac{I_i^*}{N_i^*}\right) I_i^* - \gamma_i I_i^*\right) = \sum_{i\in\Omega} \left(\beta_i \left(1 - \frac{m|L_{ii}^*|}{N_i^*}\right) - \gamma_i\right) m|L_{ii}^*| = 0$$
$$\Rightarrow \sum_{i\in\Omega} (\beta_i - \gamma_i)|L_{ii}^*| = m\left(\sum_{i\in\Omega} \beta_i \frac{|L_{ii}^*|^2}{N_i^*}\right) = m \sum_{i\in\Omega} \beta_i |L_{ii}^*| \cdot \frac{\sum\limits_{i\in\Omega} |L_{ii}^*|}{N}$$
$$\Rightarrow m = \frac{\sum\limits_{i\in\Omega} (\beta_i - \gamma_i)|L_{ii}^*|}{\sum\limits_{i\in\Omega} \beta_i |L_{ii}^*|} \cdot \frac{N}{\sum\limits_{i\in\Omega} |L_{ii}^*|} = \left(1 - \frac{1}{\mathcal{R}_0(\infty)}\right) \cdot \frac{N}{\sum\limits_{i\in\Omega} |L_{ii}^*|}$$
$$\Rightarrow T_n(\infty) = \sum_{i\in\Omega} I_i^*(\infty) = m \sum_{i\in\Omega} |L_{ii}^*| = \left(1 - \frac{1}{\mathcal{R}_0(\infty)}\right) N.$$

If $\mathcal{R}_0(\infty) < 1$, then by Lemma 3.1 the disease dies out and $T_n(\varepsilon) = 0$ for sufficiently large ε. ∎

Remark 3.4. To compare the infection sizes with fast dispersal and slow dispersal, we suppose that $\mathcal{R}_0^{(i)} > 1$ for all $i \in \Omega$. Then

$$T_n(\infty) - T_n(0) = \left(1 - \frac{1}{\mathcal{R}_0(\infty)}\right) N - \sum_{i\in\Omega} \left(1 - \frac{1}{\mathcal{R}_0^{(i)}}\right) N_i^*$$
$$= \sum_{i\in\Omega} \frac{N_i^*}{\mathcal{R}_0^{(i)}} - \frac{N}{\mathcal{R}_0(\infty)} = \left(\sum_{i\in\Omega} l_i \frac{\gamma_i}{\beta_i} - \left(\sum_{i\in\Omega} l_i \gamma_i\right) \Big/ \left(\sum_{i\in\Omega} l_i \beta_i\right)\right) N,$$

where $l_i = L_{ii}^* / \sum_{j\in\Omega} L_{jj}^*$ satisfies $0 < l_i < 1$ and $\sum_{i\in\Omega} l_i = 1$. Therefore, by using the Cauchy–Schwarz inequality, we obtain the following results:

(a) If $\beta_i = \beta$ for $i \in \Omega$, then $T_n(\infty) = T_n(0)$.
(b) If $\gamma_i = \gamma$ for $i \in \Omega$, then $T_n(\infty) \geq T_n(0)$ with equality if and only if $\beta_i = \beta$ for $i \in \Omega$.
(c) If $\beta_i - \gamma_i$ is constant for $i \in \Omega$, then $T_n(\infty) \leq T_n(0)$ with equality if and only if $\beta_i = \beta$ for $i \in \Omega$.

Biologically speaking, large dispersal results in more infections than small dispersal, provided that all patches have the same recovery rate. Thus, an increase in diffusion coefficient reduces the basic reproduction number but may enlarge the total infection size. The conclusion of part (c) can be extended to $T_n(\varepsilon) < T_n(0)$ for $\varepsilon > 0$ by calculating the tangent space of the ellipsoid $\sum_{i\in\Omega}(\beta_i(1-I_i/N_i^*)-\gamma_i)I_i = 0$ at point $(I_1^*(0),\dots,I_n^*(0))$. In addition, if L is line-sum-symmetric, then $l_i = 1/n$ for all $i \in \Omega$ and the difference becomes

$$T_n(\infty) - T_n(0) = \left(\frac{1}{n}\sum_{i\in\Omega}\frac{\gamma_i}{\beta_i} - \sum_{i\in\Omega}\gamma_i \Big/ \sum_{i\in\Omega}\beta_i\right) N.$$

Thus, it follows from Proposition A.3 in DeAngelis, Ni, and Zhang [11] that

(a) if one of the sequences $\{\mathcal{R}_0^{(i)}\}_{i\in\Omega}$ and $\{\beta_i\}_{i\in\Omega}$ is monotone increasing and the other is monotone decreasing, then $T_n(\infty) \le T_n(0)$;

(b) if both $\{\mathcal{R}_0^{(i)}\}_{i\in\Omega}$ and $\{\beta_i\}_{i\in\Omega}$ are monotone increasing or decreasing, then $T_n(\infty) \ge T_n(0)$.

By the continuity of $T_n(\varepsilon)$ in $\varepsilon \in \mathbb{R}_+$, the change trend of $T_n(\varepsilon)$ near zero can be determined by its right derivative.

THEOREM 3.5. *For model* (2.3)*, if* $\mathcal{R}_0^{(i)} \neq 1$ *for all* $i \in \Omega$*, then*

$$T_n'(0+) = \sum_{i\in\Omega}\left(\frac{1}{|\beta_i-\gamma_i|}\sum_{j\in\Omega}L_{ij}I_j^*(0)\right).$$

In particular,

$$T_2'(0+) = \left(\frac{1}{|\beta_2-\gamma_2|} - \frac{1}{|\beta_1-\gamma_1|}\right)(L_{21}I_1^*(0) - L_{12}I_2^*(0))$$

and if $\mathcal{R}_0^{(1)} > \max\{\mathcal{R}_0^{(2)}, 1\}$*, then*

$$\operatorname{sgn}(T_2'(0+)) = \operatorname{sgn}\left(\beta_1 - \gamma_1 - |\beta_2-\gamma_2|\right).$$

Proof. Suppose $\mathcal{R}_0(0) = \max_{i\in\Omega}\mathcal{R}_0^{(i)} > 1$. Otherwise, $T_n(\varepsilon) \equiv 0$ for $\varepsilon \ge 0$ and the conclusion immediately holds. Thus, for sufficiently small ε, we have $\mathcal{R}_0(\varepsilon) > 1$ and there exists a unique positive solution $(I_1^*,\dots,I_n^*)$ to the equilibrium equations

$$M_n(I_1^*,\dots,I_n^*)^T = \mathbf{0}, \tag{3.1}$$

where $M_n = F - V - \operatorname{diag}\{\beta_1 I_1^*/N_1^*,\dots,\beta_n I_n^*/N_n^*\}$. Differentiating both sides of (3.1) with respect to ε gives

$$\tilde{M}_n\left(\frac{dI_1^*}{d\varepsilon},\dots,\frac{dI_n^*}{d\varepsilon}\right)^T = -\left(\sum_{j\in\Omega}L_{1j}I_j^*,\dots,\sum_{j\in\Omega}L_{nj}I_j^*\right)^T, \tag{3.2}$$

where $\tilde{M}_n = M_n - \operatorname{diag}\{\beta_1 I_1^*/N_1^*,\dots,\beta_n I_n^*/N_n^*\}$. The essential nonnegativity and irreducibility of M_n imply that $s(M_n) = 0$ and hence $s(\tilde{M}_n) < s(M_n) = 0$ and $\operatorname{sgn}(|\tilde{M}_n|) = (-1)^n \neq 0$. So, $\tilde{M}_n^{-1}$ exists and is negative (see, e.g., Corollary 4.3.2 in Smith [35]). Solving $dI_i^*/d\varepsilon$ from (3.2) gives

$$\left(\frac{dI_1^*}{d\varepsilon},\dots,\frac{dI_n^*}{d\varepsilon}\right)^T = -\tilde{M}_n^{-1}\left(\sum_{j\in\Omega}L_{1j}I_j^*,\dots,\sum_{j\in\Omega}L_{nj}I_j^*\right)^T. \tag{3.3}$$

As $\varepsilon \to 0+$, we have

$$\begin{aligned}\tilde{M}_n &\to \operatorname{diag}\{\beta_1 - \gamma_1 - 2\beta_1 I_1^*(0)/N_1^*, \dots, \beta_n - \gamma_n - 2\beta_n I_n^*(0)/N_n^*\} \\ &= -\operatorname{diag}\{|\beta_1 - \gamma_1|, \dots, |\beta_n - \gamma_n|\}\end{aligned}$$

and hence

$$\begin{aligned}T_n'(0+) &= \left(\frac{1}{|\beta_1 - \gamma_1|}, \dots, \frac{1}{|\beta_n - \gamma_n|}\right)\left(\sum_{j\in\Omega} L_{1j} I_j^*(0), \dots, \sum_{j\in\Omega} L_{nj} I_j^*(0)\right)^T \\ &= \sum_{i\in\Omega}\left(\frac{1}{|\beta_i - \gamma_i|}\sum_{j\in\Omega} L_{ij} I_j^*(0)\right).\end{aligned}$$

For $n = 2$, if $\mathcal{R}_0^{(1)} > \mathcal{R}_0^{(2)} > 1$, then we have

$$\begin{aligned}T_2'(0+) &= \left(\frac{1}{|\beta_2 - \gamma_2|} - \frac{1}{|\beta_1 - \gamma_1|}\right)(L_{21} I_1^*(0) - L_{12} I_2^*(0)) \\ &= \frac{\beta_1 - \gamma_1 - \beta_2 + \gamma_2}{(\beta_1 - \gamma_1)(\beta_2 - \gamma_2)}\left(L_{21}\left(1 - 1/\mathcal{R}_0^{(1)}\right) N_1^* - L_{12}\left(1 - 1/\mathcal{R}_0^{(2)}\right) N_2^*\right) \\ &= \frac{\beta_1 - \gamma_1 - \beta_2 + \gamma_2}{(\beta_1 - \gamma_1)(\beta_2 - \gamma_2)}\left(\frac{1}{\mathcal{R}_0^{(2)}} - \frac{1}{\mathcal{R}_0^{(1)}}\right) L_{12} N_2^*.\end{aligned}$$

The last equality follows from $L_{21} N_1^* - L_{12} N_2^* = 0$. The case of $\mathcal{R}_0^{(1)} > 1 > \mathcal{R}_0^{(2)}$ is simpler and can be proved similarly. ∎

It is easy to show that $T_n'(0+)$ can be positive or negative for any $n \geq 2$ by constructing concrete examples (e.g., $\mathcal{R}_0^{(1)} > 1$ but $\mathcal{R}_0^{(i)} < 1$ for all $i \in \Omega\backslash\{1\}$). Based on Theorems 3.3 and 3.5, we can further construct numerical examples in which the asymptotic total infection size is not a monotone function of the diffusion coefficient.

COROLLARY 3.6. *For model* (2.3)*, if* $T_n(0) \leq T_n(\infty)$ *and* $T_n'(0+) < 0$*, or* $T_n(0) \geq T_n(\infty)$ *and* $T_n'(0+) > 0$*, then* $T_n(\varepsilon)$ *nonmonotonically depends on* ε*.*

The remainder of this section focuses on the impact of dispersal on the distribution of infections or disease prevalence of each individual patch, i.e., $I_i^*(\varepsilon)$ or $I_i^*(\varepsilon)/N_i^*$ for $i \in \Omega$. We are particularly interested in studying whether a high-risk patch still has high disease prevalence in the presence of population dispersal. The following lower and upper bounds on the I-component of the endemic equilibrium E^* comes from Lemma 3.1 in Gao and Ruan [21], which was proved by applying the theory of monotone dynamical systems (in particular Proposition 3.2.1 and Theorem 4.1.1 in Smith [35]). It partially generalizes Proposition 1 in Arditi, Lobry, and Sari [3] from two-patch to n-patch.

LEMMA 3.7. *For model* (2.3)*, if* $\mathcal{R}_0(\varepsilon) > 1$ *for* $\varepsilon > 0$*, then there exists a globally asymptotically stable endemic equilibrium* $E^* = (\boldsymbol{N}^* - \boldsymbol{I}^*(\varepsilon), \boldsymbol{I}^*(\varepsilon))$ *satisfying*

$$\left(\min_{i\in\Omega}\frac{I_i^*(0)}{|L_{ii}^*|}\right)|L_{jj}^*| < I_j^*(\varepsilon) < \left(\max_{i\in\Omega}\frac{I_i^*(0)}{|L_{ii}^*|}\right)|L_{jj}^*|,\ j \in \Omega,$$

where $I_i^*(0) = (1 - 1/\mathcal{R}_0^{(i)})^+ N_i^*$ *for* $i \in \Omega$*. If, in addition,* L *is line-sum-symmetric, then*

$$\min_{i\in\Omega} I_i^*(0) < I_j^*(\varepsilon) < \max_{i\in\Omega} I_i^*(0),\ j \in \Omega,$$

where $I_i^*(0) = (1 - 1/\mathcal{R}_0^{(i)})^+ N/n$ *for* $i \in \Omega$.

Since $(N_1^*, \dots, N_n^*)$ is proportional to $(L_{11}^*, \dots, L_{nn}^*)$, rewriting the first inequality in Lemma 3.7 gives an estimate of the disease prevalence of each patch as follows. Note that the estimate also works for the disease prevalence over all patches, i.e., $T_n(\varepsilon)/N$.

PROPOSITION 3.8. *For model* (2.3)*, if* $\mathcal{R}_0(\varepsilon) > 1$ *for* $\varepsilon > 0$*, then the disease prevalence at the endemic equilibrium* $E^* = (\boldsymbol{N}^* - \boldsymbol{I}^*(\varepsilon), \boldsymbol{I}^*(\varepsilon))$ *satisfies*

$$\left(1 - \frac{1}{\min\limits_{i\in\Omega} \mathcal{R}_0^{(i)}}\right)^+ < \frac{I_j^*(\varepsilon)}{N_j^*} < 1 - \frac{1}{\max\limits_{i\in\Omega} \mathcal{R}_0^{(i)}},\ j \in \Omega.$$

The disease prevalence of patch i in isolation is $\max\{1 - 1/\mathcal{R}_0^{(i)}, 0\}$, which means that without diffusion a higher risk patch has higher disease prevalence. The above result indicates that diffusion decreases the disease prevalence and infection size of the highest risk patch but increases those of the lowest risk patch. Can the highest risk patch have the lowest disease prevalence or the lowest risk patch have the highest disease prevalence in the presence of diffusion? We find that this extreme scenario cannot happen for model (2.3). Thus, the sequence of the disease prevalences of each patch cannot be in the descending order of the patch reproduction numbers.

THEOREM 3.9. *For model* (2.3)*, suppose that* $\mathcal{R}_0^{(1)} \geq \cdots \geq \mathcal{R}_0^{(n)}$ *and* $\mathcal{R}_0(\varepsilon) > 1$ *for* $\varepsilon > 0$*. Then the disease prevalence at the endemic equilibrium* $E^* = (\boldsymbol{N}^* - \boldsymbol{I}^*(\varepsilon), \boldsymbol{I}^*(\varepsilon))$ *satisfies*

$$\frac{I_1^*(\varepsilon)}{N_1^*} > \min_{i\in\Omega} \frac{I_i^*(\varepsilon)}{N_i^*} \quad \textit{and} \quad \frac{I_n^*(\varepsilon)}{N_n^*} < \max_{i\in\Omega} \frac{I_i^*(\varepsilon)}{N_i^*}.$$

In particular, for the two-patch case, we have $I_1^*(\varepsilon)/N_1^* > I_2^*(\varepsilon)/N_2^*$*, i.e., the disease prevalence of the high-risk patch is always larger than that of the low-risk patch.*

Proof. We only prove the first part, while the second part can be shown similarly. Suppose not, i.e., the inequality $I_1^*(\varepsilon)/N_1^* > \min_{i\in\Omega} I_i^*(\varepsilon)/N_i^*$ may fail; then there exists some $\varepsilon_0 > 0$ such that $I_1^*(\varepsilon_0)/N_1^* = \min_{i\in\Omega} I_i^*(\varepsilon_0)/N_i^*$.

Claim: $I_1^*(\varepsilon)/N_1^* = \cdots = I_n^*(\varepsilon)/N_n^*$ if and only if $\mathcal{R}_0^{(1)} = \cdots = \mathcal{R}_0^{(n)}$. Suppose $I_i^*(\varepsilon)/N_i^* = \tau \in (0, 1)$ for all $i \in \Omega$. Then

$$\sum_{j\in\Omega} L_{ij} I_j^* = \sum_{j\in\Omega} L_{ij} \tau N_j^* = \tau \sum_{j\in\Omega} L_{ij} N_j^* = 0,\ i \in \Omega,$$

which implies that

$$f_i(I_i^*) := \beta_i \left(1 - \frac{I_i^*}{N_i^*}\right) I_i^* - \gamma_i I_i^* = 0 \Rightarrow \frac{I_i^*}{N_i^*} = 1 - \frac{\gamma_i}{\beta_i} = 1 - \frac{1}{\mathcal{R}_0^{(i)}} = \tau,\ i \in \Omega.$$

Hence $\mathcal{R}_0^{(i)} = 1/(1 - \tau)$ for all $i \in \Omega$. On the other hand, if $\mathcal{R}_0^{(1)} = \cdots = \mathcal{R}_0^{(n)}$, then $\mathcal{R}_0 = \mathcal{R}_0^{(1)} > 1$ and the unique positive solution to (2.5) is $\boldsymbol{I}^* = (1 - 1/\mathcal{R}_0)\boldsymbol{N}^*$, or equivalently, $I_i^*/N_i^* = 1 - 1/\mathcal{R}_0$ for $i \in \Omega$.

It follows from the above claim and the fact

$$\sum_{i\in\Omega} \left(f_i(I_i^*) + \varepsilon \sum_{j\in\Omega} L_{ij} I_j^* \right) = \sum_{i\in\Omega} f_i(I_i^*) = 0$$

that there exist $k, l \in \Omega$ such that $f_k(I_k^*) > 0$ and $f_l(I_l^*) < 0$. Thus,

$$\max_{i\in\Omega}\left(\operatorname{sgn}(\beta_i-\gamma_i)\left(1-\frac{I_i^*}{N_i^*}\cdot\frac{1}{1-1/\mathcal{R}_0^{(i)}}\right)\right)=1-\frac{I_1^*}{N_1^*}\cdot\frac{1}{1-1/\mathcal{R}_0^{(1)}},$$

which implies that

$$(\beta_1-\gamma_1)\left(1-\frac{I_1^*}{N_1^*}\cdot\frac{1}{1-1/\mathcal{R}_0^{(1)}}\right)I_1^*=\beta_1\left(1-\frac{I_1^*}{N_1^*}\right)I_1^*-\gamma_1 I_1^*=f_1(I_1^*)>0.$$

On the other hand, it follows from $L(\boldsymbol{N}^*)^T=\mathbf{0}$ that

$$\sum_{j\in\Omega}L_{1j}I_j^*\geq\sum_{j\in\Omega}L_{1j}\frac{I_1^*}{N_1^*}N_j^*=\frac{I_1^*}{N_1^*}\sum_{j\in\Omega}L_{1j}N_j^*=0.$$

So the left-hand side of the equilibrium equation for I_1 is positive, a contradiction. ∎

Remark 3.10. When three or more patches are concerned, we will numerically show that the highest/lowest risk patch does not necessarily have the highest/lowest disease prevalence even if the connectivity matrix L is symmetric. Moreover, the disease prevalence of every patch converges to the same limit for infinite diffusion, i.e., $I_i^*(\varepsilon)/N_i^* \to (1-1/\mathcal{R}_0(\infty))^+$ as $\varepsilon\to\infty$ for all $i\in\Omega$.

Remark 3.11. Dispersal changes the coordinates of the stable equilibrium, i.e., $(I_1^*(\varepsilon),\dots,I_n^*(\varepsilon)) \neq (I_1^*(0),\dots,I_n^*(0))$ for any $\varepsilon>0$, and the asymptotic disease prevalence of at least one patch unless the disease dies out in each isolated patch. In fact, it suffices to prove the case where the disease persists in all isolated patches, i.e., $\mathcal{R}_0^{(i)}>1$ for all $i\in\Omega$. If not, then for some movement strategy L and diffusion coefficient $\varepsilon>0$, we have

$$\frac{I_i^*(\varepsilon)}{N_i^*}=\frac{I_i^*(0)}{N_i^*}=1-\frac{1}{\mathcal{R}_0^{(i)}}\ \ \forall i\in\Omega,$$

and hence

$$f_i(I_i^*(\varepsilon))=0\Leftrightarrow\sum_{j\in\Omega}L_{ij}I_j^*(\varepsilon)=0\ \ \forall i\in\Omega.$$

Thus, $I_i^*(\varepsilon)/N_i^*$ is constant in $i\in\Omega$. The claim in the proof of Theorem 3.9 implies that $\mathcal{R}_0^{(i)}$ is also constant, which contradicts assumption (B3). Note that the claim also means that the distribution of the disease prevalences across the environment is nonuniform, and there does not exist an "ideal free distribution" strategy such that the distribution of infections is proportional to its host abundance. For the multipatch logistic population model in ecology, the distribution of organisms can be proportional to its resource level under any ideal free distribution strategy [16]. The difference comes from the restriction that the "carrying capacity" of the SIS patch model without dispersal, $I_i^*(0)$, depends on the movement strategy.

Remark 3.12. The patch with the highest infection risk has more exported infections than imported infections, while the patch with the lowest infection risk has more imported infections than exported infections. Mathematically speaking, suppose that $\mathcal{R}_0^{(1)}\geq\cdots\geq\mathcal{R}_0^{(n)}$ and $\mathcal{R}_0(\varepsilon)>1$ for $\varepsilon>0$. Then

$$\sum_{j\in\Omega}L_{1j}I_j^*(\varepsilon)<0\ \text{ and }\ \sum_{j\in\Omega}L_{nj}I_j^*(\varepsilon)>0.$$

In fact, it follows from Proposition 3.8 that

$$\frac{I_1^*}{N_1^*} < 1 - \frac{1}{\mathcal{R}_0^{(1)}} \Leftrightarrow -\varepsilon \sum_{i\in\Omega} L_{1j} I_j^* = f_1(I_1^*) = \beta_1 \left(1 - \frac{1}{\mathcal{R}_0^{(1)}} - \frac{I_1^*}{N_1^*}\right) I_1^* > 0.$$

The other case can be proved in a similar way. Using this method, we can give a different but simpler proof of Theorem 3.9.

4. Two-patch case. In this section, we concentrate on the two-patch submodel

$$\begin{aligned} \frac{dI_1}{dt} &= \beta_1 \left(1 - \frac{I_1}{N_1^*}\right) I_1 - \gamma_1 I_1 + \varepsilon(-L_{21} I_1 + L_{12} I_2), \\ \frac{dI_2}{dt} &= \beta_2 \left(1 - \frac{I_2}{N_2^*}\right) I_2 - \gamma_2 I_2 + \varepsilon(L_{21} I_1 - L_{12} I_2). \end{aligned} \tag{4.1}$$

Without loss of generality, we suppose that $\mathcal{R}_0^{(1)} > \mathcal{R}_0^{(2)}$.

LEMMA 4.1. *For model* (4.1)*, if* $0 < T_2(\varepsilon_0) \le T_2(0)$ *for some* $\varepsilon_0 > 0$*, then* $T_2'(\varepsilon_0) < 0$*. In particular, if* $T_2'(0+) < 0$*, then* $T_2'(\varepsilon) < 0$ *for all* $\varepsilon \in (0, \infty)$ *as* $\mathcal{R}_0(\infty) \ge 1$ *(or* $(0, \varepsilon^*)$ *as* $\mathcal{R}_0(\infty) < 1$*).*

Proof. The assumption $T_2(\varepsilon_0) > 0$ for $\varepsilon_0 > 0$ implies that $\mathcal{R}_0(0) > 1$. Denote $r_i = |\beta_i - \gamma_i|$ and $K_i = |1 - \gamma_i/\beta_i| N_i^*$ for $i = 1, 2$. We prove the statement by considering three cases as follows.

Case (1): $\mathcal{R}_0^{(1)} > \mathcal{R}_0^{(2)} > 1$. Similar to the proof of Proposition 4 in Arditi, Lobry, and Sari [3], the equilibrium equations of system (4.1) can be written as

$$\begin{aligned} K_1 - I_1^* &= -\frac{K_1}{r_1 I_1^*} \varepsilon(-L_{21} I_1^* + L_{12} I_2^*), \\ K_2 - I_2^* &= -\frac{K_2}{r_2 I_2^*} \varepsilon(L_{21} I_1^* - L_{12} I_2^*), \end{aligned}$$

and hence

$$\begin{aligned} T_2(\varepsilon) - T_2(0) &= (I_1^* + I_2^*) - (K_1 + K_2) = \varepsilon(L_{21} I_1^* - L_{12} I_2^*) \left(\frac{K_2}{r_2 I_2^*} - \frac{K_1}{r_1 I_1^*}\right) \\ &= \frac{\varepsilon}{\frac{r_1}{K_1}\frac{r_2}{K_2} I_1^* I_2^*} (L_{21} I_1^* - L_{12} I_2^*) \left(r_1 \frac{I_1^*}{K_1} - r_2 \frac{I_2^*}{K_2}\right). \end{aligned} \tag{4.2}$$

On the other hand, differentiating the equilibrium equations with respect to ε gives

$$\left(\frac{dI_1^*}{d\varepsilon}, \frac{dI_2^*}{d\varepsilon}\right)^T = \frac{L_{21} I_1^* - L_{12} I_2^*}{|\tilde{M}_2|} \begin{pmatrix} \varepsilon L_{21} \frac{I_1^*}{I_2^*} + r_2 \frac{I_2^*}{K_2} & \varepsilon L_{12} \\ \varepsilon L_{21} & \varepsilon L_{12} \frac{I_2^*}{I_1^*} + r_1 \frac{I_1^*}{K_1} \end{pmatrix} \begin{pmatrix} -1 \\ 1 \end{pmatrix},$$

where $\tilde{M}_2$ is defined as in the proof of Theorem 3.5 with $|\tilde{M}_2| > 0$. This implies that

$$\begin{aligned} T_2'(\varepsilon) &= \frac{L_{21} I_1^* - L_{12} I_2^*}{|\tilde{M}_2|} \left(\varepsilon L_{12} \frac{I_2^*}{I_1^*} + r_1 \frac{I_1^*}{K_1} + \varepsilon L_{12} - \varepsilon L_{21} \frac{I_1^*}{I_2^*} - r_2 \frac{I_2^*}{K_2} - \varepsilon L_{21}\right) \\ &= \frac{L_{21} I_1^* - L_{12} I_2^*}{|\tilde{M}_2|} \left(r_1 \frac{I_1^*}{K_1} - r_2 \frac{I_2^*}{K_2} - \frac{\varepsilon(I_1^* + I_2^*)}{I_1^* I_2^*} (L_{21} I_1^* - L_{12} I_2^*)\right). \end{aligned}$$

Thus, if $T_2(\varepsilon_0) \le T_2(0)$, then (4.2) implies that

$$\begin{aligned} T_2'(\varepsilon_0) &\le \frac{L_{21}I_1^* - L_{12}I_2^*}{|\tilde{M}_2|}\left(-\frac{\varepsilon_0(I_1^*+I_2^*)}{I_1^*I_2^*}(L_{21}I_1^* - L_{12}I_2^*)\right) \\ &= -\frac{\varepsilon_0(I_1^*+I_2^*)}{|\tilde{M}_2|I_1^*I_2^*}(L_{21}I_1^* - L_{12}I_2^*)^2 < 0. \end{aligned}$$

The fact $L_{21}I_1^* - L_{12}I_2^* \neq 0$ follows from Theorem 3.9 or Remark 3.12.

Case (2): $\mathcal{R}_0^{(1)} > \mathcal{R}_0^{(2)} = 1$. Similarly, we obtain

$$I_1^* + I_2^* - K_1 = \frac{\varepsilon}{\frac{r_1}{K_1}\frac{\beta_2}{N_2^*}I_1^*I_2^*}(L_{21}I_1^* - L_{12}I_2^*)\left(r_1\frac{I_1^*}{K_1} - \beta_2\frac{I_2^*}{N_2^*}\right) \tag{4.3}$$

and

$$T_2'(\varepsilon) = \frac{L_{21}I_1^* - L_{12}I_2^*}{|\tilde{M}_2|}\left(r_1\frac{I_1^*}{K_1} - \beta_2\frac{I_2^*}{N_2^*} - \frac{\varepsilon(I_1^*+I_2^*)}{I_1^*I_2^*}(L_{21}I_1^* - L_{12}I_2^*)\right).$$

If $T_2(\varepsilon_0) = I_1^* + I_2^* \le T_2(0) = K_1$, then (4.3) implies that

$$T_2'(\varepsilon_0) \le -\frac{\varepsilon_0(I_1^*+I_2^*)}{|\tilde{M}_2|I_1^*I_2^*}(L_{21}I_1^* - L_{12}I_2^*)^2 < 0.$$

Case (3): $\mathcal{R}_0^{(1)} > 1 > \mathcal{R}_0^{(2)}$. Similarly, we get

$$I_1^* + I_2^* - K_1 = \frac{\varepsilon}{\frac{r_1}{K_1}\frac{r_2}{K_2}I_1^*(I_2^*+K_2)}(L_{21}I_1^* - L_{12}I_2^*)\left(r_1\frac{I_1^*}{K_1} - r_2\frac{I_2^*+K_2}{K_2}\right) \tag{4.4}$$

and

$$T_2'(\varepsilon) = \frac{L_{21}I_1^* - L_{12}I_2^*}{|\tilde{M}_2|}\left(r_1\frac{I_1^*}{K_1} - r_2\frac{I_2^*}{K_2} - \frac{\varepsilon(I_1^*+I_2^*)}{I_1^*I_2^*}(L_{21}I_1^* - L_{12}I_2^*)\right).$$

If $T_2(\varepsilon_0) = I_1^* + I_2^* \le T_2(0) = K_1$, then (4.4) implies that

$$\begin{aligned} T_2'(\varepsilon_0) &\le \frac{L_{21}I_1^* - L_{12}I_2^*}{|\tilde{M}_2|}\left(r_2 - \frac{\varepsilon_0(I_1^*+I_2^*)}{I_1^*I_2^*}(L_{21}I_1^* - L_{12}I_2^*)\right) \\ &= \frac{L_{21}I_1^* - L_{12}I_2^*}{|\tilde{M}_2|}\left(r_2 - \frac{I_1^*+I_2^*}{I_1^*I_2^*}r_2I_2^*\left(1+\frac{I_2^*}{K_2}\right)\right) < 0 \end{aligned}$$

due to $\varepsilon_0(L_{21}I_1^* - L_{12}I_2^*) = r_2I_2^*(1 + I_2^*/K_2) > 0$. This completes the proof. ∎

Note that the above proof is independent of K_1 and K_2, i.e., the restriction (2.2) on N_1^* and N_2^* is not required, so the lemma can be extended to a general two-patch population model. Based on Lemma 4.1, we can easily obtain a complete classification on when dispersal leads to more or less infections.

THEOREM 4.2. *Suppose* $\mathcal{R}_0^{(1)} > \max\{\mathcal{R}_0^{(2)}, 1\}$. *The following statements are valid:*

(a) *If* $T_2'(0+) \le 0$, *then* $T_2(\varepsilon) < T_2(0)$ *for* $\varepsilon \in (0,\infty)$.
(b) *If* $0 < T_2'(0+) \le \infty$ *and* $T_2(\infty) < T_2(0)$, *then there exists* $\hat{\varepsilon}$ *such that* $T_2(\varepsilon) > T_2(0)$ *for* $\varepsilon \in (0,\hat{\varepsilon})$, $T_2(\varepsilon) = T_2(0)$ *for* $\varepsilon = \hat{\varepsilon}$, *and* $T_2(\varepsilon) < T_2(0)$ *for* $\varepsilon \in (\hat{\varepsilon},\infty)$.
(c) *If* $T_2(\infty) \ge T_2(0)$, *then* $T_2(\varepsilon) > T_2(0)$ *for* $\varepsilon \in (0,\infty)$.

Proof. It is only left to prove the cases of $T_2'(0+)=0$ and $T_2'(0+)=\infty$; all other cases immediately follow from Lemma 4.1, the continuity of $T_2(\varepsilon)$ in $\varepsilon\in[0,\infty)$, and the continuous differentiability of $T_2(\varepsilon)$ for $0<\varepsilon\ll 1$.

If $T_2'(0+)=0$, i.e., $r_1=|\beta_1-\gamma_1|=\beta_1-\gamma_1=r_2=|\beta_2-\gamma_2|>0$, then the following hold:

(1) $\mathcal{R}_0^{(1)}>\mathcal{R}_0^{(2)}>1$. It follows from Proposition 3.8 and (4.2) that

$$\frac{I_1^*}{K_1}<1<\frac{I_2^*}{K_2}\Rightarrow r_1\frac{I_1^*}{K_1}-r_2\frac{I_2^*}{K_2}<0\Rightarrow T_2(\varepsilon)<T_2(0)\ \text{ for }\ \varepsilon\in(0,\infty).$$

(2) $\mathcal{R}_0^{(1)}>1>\mathcal{R}_0^{(2)}$. Again it follows from Proposition 3.8 and (4.4) that

$$\frac{I_1^*}{K_1}<1\Rightarrow r_1\frac{I_1^*}{K_1}-r_2\frac{I_2^*+K_2}{K_2}<0\Rightarrow T_2(\varepsilon)<T_2(0)\ \text{ for }\ \varepsilon\in(0,\infty).$$

If $T_2'(0+)=\infty$, i.e., $r_2=\beta_2-\gamma_2=0\Leftrightarrow\mathcal{R}_0^{(2)}=1$, then it follows from the fact

$$r_1\frac{I_1^*}{K_1}-\beta_2\frac{I_2^*}{N_2^*}\to r_1\frac{I_1^*(0)}{K_1}-\beta_2\frac{I_2^*(0)}{N_2^*}=r_1>0\ \text{ as }\varepsilon\to 0+,$$

equation (4.3), the continuity of $T_2(\varepsilon)$, and Lemma 4.1 that the conclusion holds. ∎

Recall that $T_2'(0+)=\left(|\beta_2-\gamma_2|^{-1}-|\beta_1-\gamma_1|^{-1}\right)(L_{21}I_1^*(0)-L_{12}I_2^*(0))$ and direct calculation yields

$$T_2(\infty)-T_2(0)=\begin{cases}\dfrac{L_{12}L_{21}(\beta_1-\beta_2)(\beta_1\gamma_2-\beta_2\gamma_1)N}{(L_{12}+L_{21})\beta_1\beta_2(\beta_1L_{12}+\beta_2L_{21})} & \text{if } \mathcal{R}_0^{(1)}>\mathcal{R}_0^{(2)}\ge 1,\\ \dfrac{L_{21}\Delta}{(L_{12}+L_{21})\beta_1(\beta_1L_{12}+\beta_2L_{21})}N & \text{if } \mathcal{R}_0^{(1)}>\mathcal{R}_0(\infty)\ge 1>\mathcal{R}_0^{(2)},\\ -\dfrac{L_{12}(\beta_1-\gamma_1)}{(L_{12}+L_{21})\beta_1}N & \text{if } \mathcal{R}_0^{(1)}>1>\mathcal{R}_0(\infty)>\mathcal{R}_0^{(2)},\end{cases}$$

where $\Delta=L_{12}\beta_1(\beta_1+\beta_2-\gamma_1-\gamma_2)-L_{12}\beta_2(\beta_1-\gamma_1)-L_{21}\beta_1(\gamma_2-\beta_2)$. We can then give a more detailed classification in terms of the patch reproduction numbers $\mathcal{R}_0^{(1)}$ and $\mathcal{R}_0^{(2)}$. In addition, a lengthy but interesting proof using a graphical method similar to that used by Arditi, Lobry, and Sari [4] is given in the appendix. Note that if $\mathcal{R}_0^{(1)}>\mathcal{R}_0^{(2)}\ge 1$, then the signs of both $T_2(\infty)-T_2(0)$ and $T_2'(0+)$ are independent of the connectivity matrix L, and hence the change pattern (beneficial or detrimental) of the total infection size $T_2(\varepsilon)$ is unaffected by the selection of L.

THEOREM 4.3. *For model* (4.1)*, we have the following:*

(a) $\mathcal{R}_0^{(1)}>\mathcal{R}_0^{(2)}>1$. *Then*

(1) *if* $\beta_1-\gamma_1\le\beta_2-\gamma_2$, *then* $T_2(\varepsilon)<T_2(0)$ *for* $\varepsilon\in(0,\infty)$ *(and* $\beta_1<\beta_2$*);*

(2) *if* $\beta_1-\gamma_1>\beta_2-\gamma_2$ *and* $\beta_1<\beta_2$, *then there exists*

$$\varepsilon_a=\frac{\beta_1\beta_2(\beta_1-\gamma_1-\beta_2+\gamma_2)}{(\beta_2-\beta_1)(L_{21}\beta_1+L_{12}\beta_2)}$$

such that $T_2(\varepsilon)>T_2(0)$ *for* $\varepsilon\in(0,\varepsilon_a)$, $T_2(\varepsilon)=T_2(0)$ *for* $\varepsilon=\varepsilon_a$, *and* $T_2(\varepsilon)<T_2(0)$ *for* $\varepsilon\in(\varepsilon_a,\infty)$*;*

(3) *if* $\beta_1\ge\beta_2$, *then* $T_2(\varepsilon)>T_2(0)$ *for* $\varepsilon\in(0,\infty)$ *(and* $\beta_1-\gamma_1>\beta_2-\gamma_2$*).*

(b) $\mathcal{R}_0^{(1)}>\mathcal{R}_0^{(2)}=1$. *Then*

(1) *if* $\beta_1 < \beta_2$, *then there exists*

$$\varepsilon_b = \frac{\beta_1\beta_2(\beta_1-\gamma_1)}{(\beta_2-\beta_1)(L_{21}\beta_1+L_{12}\beta_2)}$$

such that $T_2(\varepsilon) > T_2(0)$ *for* $\varepsilon \in (0,\varepsilon_b)$, $T_2(\varepsilon) = T_2(0)$ *for* $\varepsilon = \varepsilon_b$, *and* $T_2(\varepsilon) < T_2(0)$ *for* $\varepsilon \in (\varepsilon_b,\infty)$;

(2) *if* $\beta_1 \geq \beta_2$, *then* $T_2(\varepsilon) > T_2(0)$ *for* $\varepsilon \in (0,\infty)$.

(c) $\mathcal{R}_0^{(1)} > \mathcal{R}_0(\infty) = \frac{L_{12}\beta_1+L_{21}\beta_2}{L_{12}\gamma_1+L_{21}\gamma_2} \geq 1 > \mathcal{R}_0^{(2)}$. *Then*

(1) *if* $\beta_1-\gamma_1 \leq \gamma_2-\beta_2$, *then* $T_2(\varepsilon) < T_2(0)$ *for* $\varepsilon \in (0,\infty)$;

(2) *if* $\beta_1-\gamma_1 > \gamma_2-\beta_2$ *and* $\frac{L_{21}}{L_{12}} > \frac{L_{21}\beta_1(\beta_1+\beta_2-\gamma_1-\gamma_2)}{L_{12}\beta_2(\beta_1-\gamma_1)+L_{21}\beta_1(\gamma_2-\beta_2)}$, *then there exists*

$$\varepsilon_c = \frac{\beta_1(L_{12}\beta_2(\beta_1-\gamma_1)+L_{21}\beta_1(\gamma_2-\beta_2))(\beta_1+\beta_2-\gamma_1-\gamma_2)}{(L_{12}(\beta_1(\gamma_1+\gamma_2)-\beta_1^2-\beta_2\gamma_1)+L_{21}\beta_1(\gamma_2-\beta_2))(L_{21}\beta_1+L_{12}\beta_2)}$$

such that $T_2(\varepsilon) > T_2(0)$ *for* $\varepsilon \in (0,\varepsilon_c)$, $T_2(\varepsilon) = T_2(0)$ *for* $\varepsilon = \varepsilon_c$, *and* $T_2(\varepsilon) < T_2(0)$ *for* $\varepsilon \in (\varepsilon_c,\infty)$;

(3) *if* $\frac{L_{21}}{L_{12}} \leq \frac{L_{21}\beta_1(\beta_1+\beta_2-\gamma_1-\gamma_2)}{L_{12}\beta_2(\beta_1-\gamma_1)+L_{21}\beta_1(\gamma_2-\beta_2)}$, *then* $T_2(\varepsilon) > T_2(0)$ *for* $\varepsilon \in (0,\infty)$ *(and* $\beta_1-\gamma_1 > \gamma_2-\beta_2$*).*

(d) $\mathcal{R}_0^{(1)} > 1 > \mathcal{R}_0(\infty) = \frac{L_{12}\beta_1+L_{21}\beta_2}{L_{12}\gamma_1+L_{21}\gamma_2} > \mathcal{R}_0^{(2)}$. *There exists*

$$\varepsilon^* = \frac{(\beta_1-\gamma_1)(\beta_2-\gamma_2)}{(\beta_1-\gamma_1)L_{12}+(\beta_2-\gamma_2)L_{21}} > 0$$

such that $\mathcal{R}_0(\varepsilon) > 1$ *for* $\varepsilon \in [0,\varepsilon^*)$, $\mathcal{R}_0(\varepsilon^*) = 1$ *and* $\mathcal{R}_0(\varepsilon) < 1$ *for* $\varepsilon \in (\varepsilon^*,\infty)$. *Then*

(1) *if* $\beta_1-\gamma_1 \leq \gamma_2-\beta_2$, *then* $0 < T_2(\varepsilon) < T_2(0)$ *for* $\varepsilon \in (0,\varepsilon^*)$ *and* $T_2(\varepsilon) \equiv 0$ *for* $\varepsilon \in [\varepsilon^*,\infty)$;

(2) *if* $\beta_1-\gamma_1 > \gamma_2-\beta_2$, *then* $T_2(\varepsilon) > T_2(0)$ *for* $\varepsilon \in (0,\varepsilon_c)$, $T_2(\varepsilon) = T_2(0)$ *for* $\varepsilon = \varepsilon_c$, $0 < T_2(\varepsilon) < T_2(0)$ *for* $\varepsilon \in (\varepsilon_c,\varepsilon^*)$, *and* $T_2(\varepsilon) \equiv 0$ *for* $\varepsilon \in [\varepsilon^*,\infty)$.

(e) $1 \geq \mathcal{R}_0^{(1)} > \mathcal{R}_0^{(2)}$. *Then* $T_2(\varepsilon) \equiv T_2(0) = 0$ *for* $\varepsilon \in [0,\infty)$.

It is worth noting that the analysis performed by Arditi, Lobry, and Sari [3, 4] is limited to a source-source system (i.e., $r_1 = \beta_1-\gamma_1 > 0$ and $r_2 = \beta_2-\gamma_2 > 0$). We extensively generalize their findings by using both the analytical and graphical methods.

5. Numerical simulations. We further explore how dispersal affects the total infection size in a numerical way. The parameter ranges are mainly based on the common cold by choosing $\beta_i \in [0.05, 0.3]$ and $\gamma_i \in [0.05, 0.15]$ with per day as the time unit [38]. For convenience, we assume the total population size $N = 1$, which makes $T_n(\varepsilon)$ equivalent to the overall disease prevalence.

Example 5.1 (dependence of total infection size on diffusion coefficient). For the two-patch submodel (4.1), choosing four parameter sets as listed in Table 1, we plot the curves of T_2 and $\mathcal{R}_0$ in terms of $\varepsilon \in [0,1]$ in Figure 1. In all four scenarios, two source patches, with patch 1 being the high-risk patch, are considered, i.e., $\mathcal{R}_0^{(1)} > \mathcal{R}_0^{(2)} > 1$. As indicated by Lemma 3.1, the basic reproduction number $\mathcal{R}_0$ is always strictly decreasing and strictly convex in the dispersal rate ε. In the first scenario, it follows from Theorem 4.2 that the negativity of $T_2'(0+) = -0.049$ implies that $T_2(\varepsilon)$ decreases strictly from $T_2(0) = 0.37$ to $T_2(\infty) = 0.33$ (see Figure 1(a)). Namely, fast diffusion

reduces the transmission potential and the infection size simultaneously. In the second and third scenarios, the fact that $T_2'(0+) > 0$ and $T_2(0) < T_2(\infty)$ means that dispersal always leads to larger total infection size than no dispersal. More specifically, $T_2(\varepsilon)$ initially increases then decreases in scenario 2 but constantly increases in scenario 3 (see Figures 1(b) and 1(c)). The third scenario is of particular interest in that increasing diffusion always has inconsistent effects from the aspects of infection risk and infection size, respectively. The last scenario has $T_2'(0+) > 0$ and $T_2(0) > T_2(\infty)$, which suggests that small dispersal is detrimental but large dispersal is beneficial (see Figure 1(d)). Similar scenarios can be found when dispersal is asymmetric.

TABLE 1
The parameter settings for Figure 1 with $L_{12} = L_{21} = 1$ for all scenarios.

	β_1	γ_1	β_2	γ_2	$\mathcal{R}_0^{(1)}$	$\mathcal{R}_0^{(2)}$	$\mathcal{R}_0(\infty)$	$T_2(0)$	$T_2(\infty)$	$T_2'(0+)$
a	0.1	0.051	0.2	0.15	1.96	1.33	1.49	0.37	0.33	−0.049
b	0.25	0.15	0.15	0.14	1.67	1.07	1.38	0.23	0.275	15
c	0.24	0.12	0.16	0.1	2	1.6	1.82	0.44	0.45	0.52
d	0.1	0.06	0.15	0.14	1.67	1.07	1.25	0.23	0.2	12.5

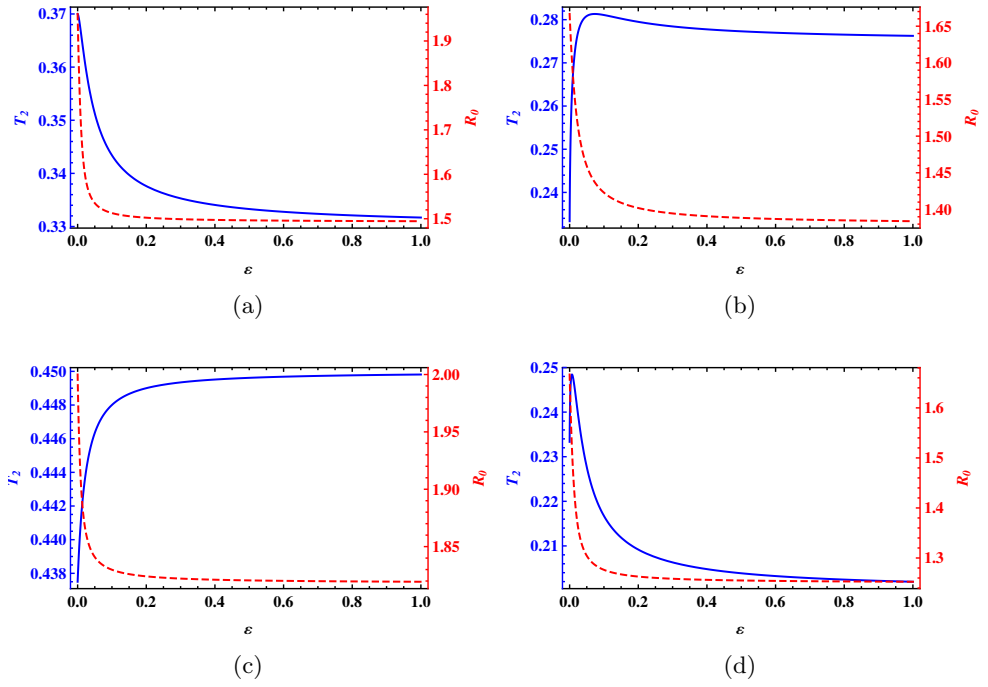

FIG. 1. *The total number of infections T_2 (solid line) and the basic reproduction number $\mathcal{R}_0$ (dashed line) versus diffusion coefficient ε under four scenarios. The x-axis represents ε, while the left and right y-axes represent T_2 and $\mathcal{R}_0$, respectively. See Table 1 for parameter settings.*

Briefly speaking, there are four types of relationships between the total infection size and diffusion coefficient for the two-patch submodel, i.e., strictly decreasing, initially increasing and then decreasing, strictly increasing, and constant. More complex dependencies can appear when three or more patches are concerned (see Figure 2 for the three-patch case).

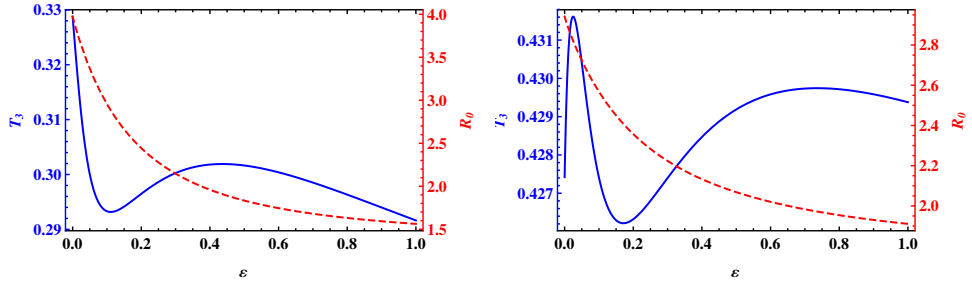

(a) (b)

FIG. 2. *The total number of infections T_3 (solid line) and the basic reproduction number $\mathcal{R}_0$ (dashed line) versus diffusion coefficient ε under two scenarios. The x-axis represents ε, while the left and right y-axes represent T_3 and $\mathcal{R}_0$, respectively. Parameter values are* (a) $\beta_1 = 0.29$, $\gamma_1 = 0.073$, $\beta_2 = 0.105$, $\gamma_2 = 0.061$, $\beta_3 = 0.053$, $\gamma_3 = 0.14$, $L_{12} = 0.03$, $L_{13} = 0.094$, $L_{21} = 0.176$, $L_{23} = 0.66$, $L_{31} = 0.098$, $L_{32} = 0.52$; (b) $\beta_1 = 0.25$, $\gamma_1 = 0.085$, $\beta_2 = 0.131$, $\gamma_2 = 0.053$, $\beta_3 = 0.076$, $\gamma_3 = 0.135$, $L_{12} = 0.14$, $L_{13} = 0.04$, $L_{21} = 0.13$, $L_{23} = 0.47$, $L_{31} = 0.04$, $L_{32} = 0.45$.

Example 5.2 (disease persistence versus disease prevalence). Consider a two-patch environment with the same parameter setting as scenario 2 in Table 1. The curves of the disease prevalences of patch 1, patch 2, and both patches in terms of diffusion coefficient, i.e.,

$$\frac{I_1^*(\varepsilon)}{N_1^*}, \quad \frac{I_2^*(\varepsilon)}{N_2^*}, \quad \text{and} \quad \frac{I_1^*(\varepsilon) + I_2^*(\varepsilon)}{N_1^* + N_2^*} = \frac{T_2(\varepsilon)}{N},$$

are plotted in Figure 3(a). Since $\mathcal{R}_0^{(1)} = 1.67$ and $\mathcal{R}_0^{(2)} = 1.07$, the disease prevalences of patches 1 and 2 in isolation are, respectively,

$$\frac{I_1^*(0)}{N_1^*} = 1 - \frac{1}{\mathcal{R}_0^{(1)}} = 0.4 \quad \text{and} \quad \frac{I_2^*(0)}{N_2^*} = 1 - \frac{1}{\mathcal{R}_0^{(2)}} = 0.067.$$

When the two patches are connected, the disease prevalence of patch 1 decreases, while that of patch 2 increases as diffusion coefficient ε varies from 0 to ∞. The sequence of the three curves from top to bottom are for patch 1, both patches, and patch 2, respectively. In other words, the disease prevalence of the high-risk patch is constantly higher than that of the low-risk patch, and the overall disease prevalence is between them. As $\varepsilon \to \infty$, all three disease prevalences converge to the same value, $1 - 1/\mathcal{R}_0(\infty)$. However, for a three-patch environment as illustrated in Figure 3(b), the lowest risk patch does not necessarily have the lowest disease prevalence whenever the dispersal rate is large enough. So the disease prevalences may not be in ascending order of the patch reproduction numbers even if the connectivity matrix L is symmetric. A possible reason for the occurrence of this phenomenon is that the connection between the lowest risk and the highest risk patches is much stronger than any other connection, which results in more cases imported to the lowest risk patch. With a similar idea, one can easily construct an example in which the highest risk patch does not have the highest disease prevalence.

Example 5.3 (effect of asymmetric dispersal). The total infection size, or equivalently, the overall disease prevalence, is not only affected by spatial heterogeneity and diffusion coefficient, but it is also influenced by patch connectivity. Using the same parameter set as the last scenario in Table 1, the contour plot in Figure 4(a) shows

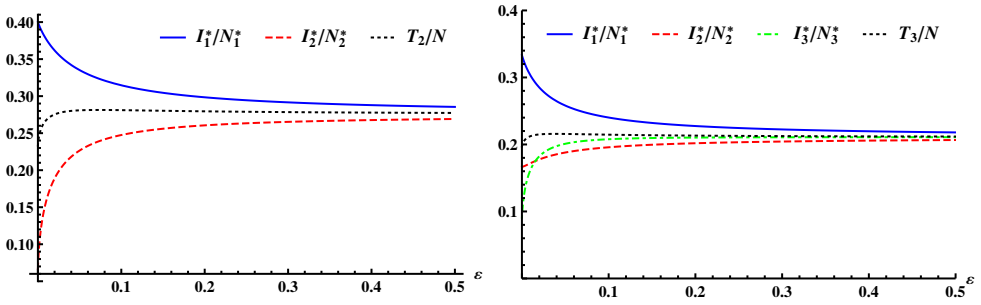

(a) (b)

FIG. 3. *The single-patch and overall disease prevalences versus diffusion coefficient. Parameter settings are* (a) $\beta_1 = 0.25$, $\gamma_1 = 0.15$, $\beta_2 = 0.15$, $\gamma_2 = 0.14$, $L_{12} = L_{21} = 1$ *for a two-patch environment;* (b) $\beta_1 = 0.15$, $\beta_2 = 0.12$, $\beta_3 = 0.11$, $\gamma_1 = \gamma_2 = \gamma_3 = 0.1$, $L_{12} = L_{21} = 0.1$, $L_{13} = L_{31} = 0.9$, $L_{23} = L_{32} = 0.2$ *for a three-patch environment.*

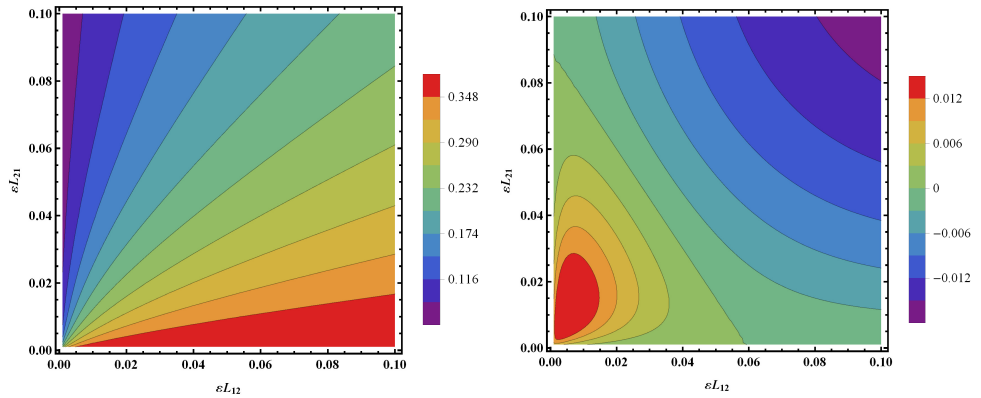

(a) (b)

FIG. 4. *The contour plots of the total infection size* $T_2(\varepsilon L_{12}, \varepsilon L_{21})$ *(left panel) and the difference of the total infection sizes with and without diffusion* $T_2(\varepsilon L_{12}, \varepsilon L_{21}) - T_2(0,0)$ *(right panel) versus travel rates* εL_{12} *and* εL_{21}. *Parameter values are* $\beta_1 = 0.1$, $\gamma_1 = 0.06$, $\beta_2 = 0.15$, $\gamma_2 = 0.14$.

the total infection size versus travel rates εL_{12} and εL_{21}. We observe that if both the diffusion coefficient ε and the asymmetry L_{ij}/L_{ji} are large enough, then the overall disease prevalence approaches the disease prevalence of patch i in isolation. In fact, for the two-patch case, if $\mathcal{R}_0(\infty) > 1$, then it follows from Theorem 3.3 that

$$\frac{T_2(\infty)}{N} = 1 - \frac{1}{\mathcal{R}_0(\infty)} = 1 - \frac{\gamma_1 L_{11}^* + \gamma_2 L_{22}^*}{\beta_1 L_{11}^* + \beta_2 L_{22}^*} = 1 - \frac{\gamma_1 L_{12} + \gamma_2 L_{21}}{\beta_1 L_{12} + \beta_2 L_{21}}$$
$$= 1 - \frac{\gamma_1 + L_{21}/L_{12}\gamma_2}{\beta_1 + L_{21}/L_{12}\beta_2} \approx \begin{cases} 1 - \frac{1}{\mathcal{R}_0^{(1)}} & \text{if } \frac{L_{12}}{L_{21}} \gg 1, \\ 1 - \frac{1}{\mathcal{R}_0^{(2)}} & \text{if } \frac{L_{21}}{L_{12}} \gg 1. \end{cases}$$

In addition, the total infection size decreases with respect to the travel rate from high-risk patch to low-risk patch, L_{21}, but increases with respect to the travel rate from low-risk patch to high-risk patch, L_{12}. Meanwhile, the difference of the total numbers

of infections with and without dispersal is big when the asymmetry is not very large and the diffusion coefficient is relatively small or sufficiently large (see Figure 4(b)).

6. Discussion. Despite a large number of studies regarding the effect of human movement on the spread and control of infectious diseases, very few of them have been focused on how population dispersal affects the size and distribution of infections. In this paper, we considered an SIS patch model where the disease does not impair the mobility of infected people. Either the disease-free equilibrium or the endemic equilibrium is globally attractive. The numbers of infections in each patch and over all patches at the globally stable equilibrium are obtained as the diffusion coefficient goes to zero or infinity. We established sufficient conditions under which large dispersal causes more or less infections than no dispersal. The right derivative of the total infection size at zero was calculated to determine its change trend for small dispersal. We estimated the number of infections and the disease prevalence of each patch at any dispersal rate and showed that diffusion reduces the infection size and disease prevalence of the highest risk patch but increases these of the lowest risk patch. However, the highest/lowest risk patch cannot have the lowest/highest disease prevalence. In the case of two patches, the disease is always more prevalent in the high-risk patch than the low-risk patch. Furthermore, we gave a complete classification on when dispersal has a beneficial or detrimental effect on reducing infections across two patches.

In addition, numerical simulations were conducted to further investigate how disease morbidity and endemic level vary with human migration. In the first example, we confirmed that for the two-patch submodel the change pattern of the total infection size in diffusion coefficient is completely governed by the total infection size and its right derivative at no dispersal and the infection size with infinite dispersal. Specifically, the total infection size either decreases, increases, or initially increases then decreases with respect to diffusion coefficient. There are more change patterns for the model involved more patches. The second example examined the relationship between infection risk and disease prevalence. Higher infection risk means higher disease prevalence for the two-patch case. However, this result may fail under suitable travel patterns for an environment containing three or more patches. The last example concerned the impact of dispersal asymmetry. We found that the asymmetry can significantly affect the persistence and endemicity of infectious diseases.

The basic reproduction number only characterizes initial transmission and serves as a threshold quantity between disease persistence and extinction. It is usually very difficult or even impossible to eradicate an infectious disease due to natural reservoir, imported cases, pathogen mutation, etc. Therefore, reducing the number of infections is a more feasible objective for the global control of most infectious diseases. The potential inconsistency between the basic reproduction number and the total infection size indicates that inappropriate border control may change the disease persistence and disease prevalence in an opposite direction. To design a better control strategy, health agencies should consider the influence of population dispersal on both infection risk and infection size. Moreover, limiting human movement can lead to more infections under certain conditions. This possibility deserves much attention for the COVID-19 pandemic, in which domestic or international travel restrictions including lockdowns are widely carried out across the globe.

To the best knowledge of the author, this is possibly the first theoretical work about the effect of human movement on disease burden and its distribution. There are many directions to improve and extend the current work. It is generally unknown how

the total infection size changes with medium diffusion coefficient. We are interested in developing a systematic approach to classify the parameter space into beneficial and detrimental parts for a model system with an arbitrary number of patches. The graphical method used for the two-patch case can hardly be applied to cases with three or more patches since the associated ellipse, parabola, and line in the plane become ellipsoid, paraboloid, and hyperplane in higher dimensional space. Under what level of diffusion does the total infection size attain its maximum or minimum? To what extent can diffusion change the total infection size relative to no dispersal for a given connectivity matrix? When the susceptible and infected subpopulations have different diffusion coefficients, Allen et al. [1] and Chen et al. [8], respectively, showed the existence and uniqueness of the endemic equilibrium if the connectivity matrix is symmetric and asymmetric. We would like to know whether the main results obtained in this paper still hold [19]. Similar questions can be considered for the SIS patch models with vital dynamics [20, 42, 43], the SIR patch model [29], the SEIR or SEIRS patch model [34], the multipatch Ross–Macdonald model [9, 22], the SIS reaction-diffusion model [2], and so on. In reality, movement from high-risk patch to low-risk patch may be restricted or banned. For example, the United States banned travel from China very early to fight the novel coronavirus, but it failed to block imported cases from Europe. What happens to the total infection size and its distribution if some but not all travel rates are proportionally decreasing or increasing while the remainder are unchanged [21]? The methods and results developed in this topic may be valuable in studying the effect of dispersal on total population abundance in spatial ecology.

Appendix: Proof of Theorem 4.3.

Proof. The positive equilibrium (I_1^*, I_2^*) of system (4.1) is the solution to

$$\begin{aligned} &\beta_1\left(1-\frac{I_1}{N_1^*}\right)I_1-\gamma_1 I_1+\varepsilon(-L_{21}I_1+L_{12}I_2)=0,\\ &\beta_2\left(1-\frac{I_2}{N_2^*}\right)I_2-\gamma_2 I_2+\varepsilon(L_{21}I_1-L_{12}I_2)=0. \end{aligned} \tag{A1}$$

Adding the two equations in (A1) and solving I_2 from the first equation of (A1) yields

$$\begin{aligned} &\mathscr{E}(I_1,I_2):\beta_1\left(1-\frac{I_1}{N_1^*}\right)I_1-\gamma_1 I_1+\beta_2\left(1-\frac{I_2}{N_2^*}\right)I_2-\gamma_2 I_2=0,\\ &\mathscr{P}(I_1):I_2=\frac{L_{21}}{L_{12}}I_1-\frac{1}{\varepsilon L_{12}}\left(\beta_1\left(1-\frac{I_1}{N_1^*}\right)I_1-\gamma_1 I_1\right), \end{aligned} \tag{A2}$$

where $\mathscr{E}$ is an ellipse independent of ε and $\mathscr{P}$ is a parabola (open upward). Obviously, systems (A1) and (A2) are equivalent. Further, if $\mathcal{R}_0^{(1)} > 1$, then $\mathscr{P}$ can be written as

$$\mathscr{P}_\varepsilon(I_1):I_2=\frac{L_{21}}{L_{12}}I_1-\frac{r_1}{\varepsilon L_{12}}\left(1-\frac{I_1}{K_1}\right)I_1,$$

where $r_1=\beta_1-\gamma_1>0$ and $K_1=I_1^*(0)=(1-\gamma_1/\beta_1)N_1^*>0$. The parabola $\mathscr{P}_\varepsilon$ passes through $O(0,0)$ and $M(K_1, K_1L_{21}/L_{12})$ for any $\varepsilon>0$. Moreover, the left and right branches of the parabola $\mathscr{P}_\varepsilon$ converge, respectively, to vertical lines $I_1=0$ and $\mathscr{P}_0: I_1=K_1$ as $\varepsilon\to 0+$, and to a straight line $\mathscr{P}_\infty:\ I_2=\frac{L_{21}}{L_{12}}I_1$ as $\varepsilon\to\infty$.

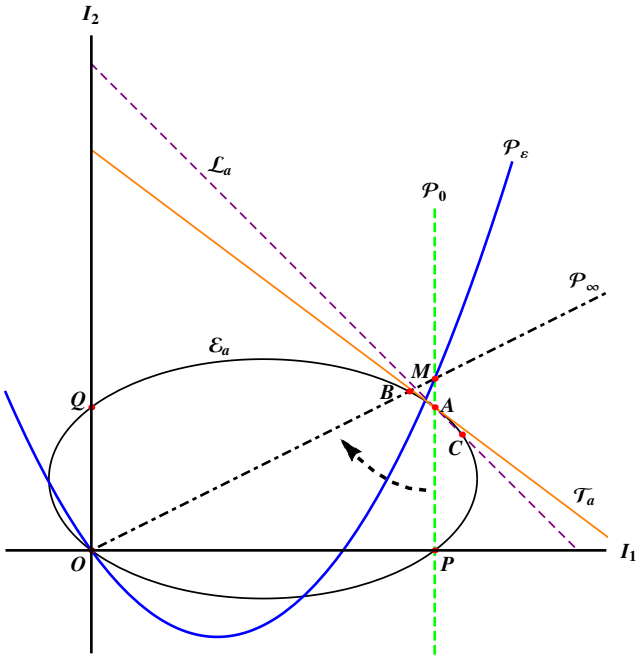

FIG. A1. *A schematic graph for Case* (a2).

Case (a): $\mathcal{R}_0^{(1)} > \mathcal{R}_0^{(2)} > 1$. Denote $r_2 = \beta_2 - \gamma_2 > 0$ and $K_2 = I_2^*(0) = (1 - \gamma_2/\beta_2)N_2^* > 0$. Then the ellipse $\mathscr{E}$ can be rewritten as

$$\mathscr{E}_a(I_1, I_2) : r_1 \left(1 - \frac{I_1}{K_1}\right) I_1 + r_2 \left(1 - \frac{I_2}{K_2}\right) I_2 = 0.$$

Clearly, $\mathscr{E}_a$ passes through the points $O(0,0)$, $P(K_1,0)$, $A(K_1,K_2)$, and $Q(0,K_2)$. As ε varies from 0 to ∞, the intersection of $\mathscr{E}_a$ and the parabola $\mathscr{P}_\varepsilon$ moves along the ellipse from A to

$$B = \left(\frac{L_{12}K_1K_2(r_1L_{12} + r_2L_{21})}{r_1K_2L_{12}^2 + r_2K_1L_{21}^2}, \frac{L_{21}K_1K_2(r_1L_{12} + r_2L_{21})}{r_1K_2L_{12}^2 + r_2K_1L_{21}^2} \right),$$

which is the nontrivial intersection of $\mathscr{E}_a$ and $\mathscr{P}_\infty$ (see Figure A1).

To facilitate comparison of $T_2(\varepsilon)$ and $T_2(0) = I_1^*(0) + I_2^*(0) = K_1 + K_2$, we define a straight line $\mathscr{L}_a : I_1 + I_2 = K_1 + K_2$. If the intersection of the ellipse $\mathscr{E}_a$ and the parabola $\mathscr{P}_\varepsilon$, i.e., (I_1^*, I_2^*), is on or below the line $\mathscr{L}_a$, then $T_2(\varepsilon) \le T_2(0)$, whereas if the intersection is above the line, then $T_2(\varepsilon) > T_2(0)$. Direct calculation finds that the ellipse $\mathscr{E}_a$ and the line $\mathscr{L}_a$ have two intersections:

$$A(K_1, K_2) \quad \text{and} \quad C\left(\frac{r_2K_1(K_1 + K_2)}{r_1K_2 + r_2K_1}, \frac{r_1K_2(K_1 + K_2)}{r_1K_2 + r_2K_1} \right).$$

By differentiating the equation of $\mathscr{E}_a$ with respect to I_1 and substituting point A into the resulting equation, the slope of $\mathscr{T}_a$, the tangent line to the ellipse $\mathscr{E}_a$ at point A, is $-\frac{r_1}{r_2}$. Next we split the model parameter space in terms of the relative position of the three points A, B, and C, or equivalently, the three lines $\overrightarrow{OA}$, $\overrightarrow{OB}$, and $\overrightarrow{OC}$ whose

slopes are

$$\frac{K_2}{K_1}, \quad \frac{L_{21}}{L_{12}}, \quad \text{and} \quad \frac{r_1K_2}{r_2K_1},$$

respectively. It follows from

$$\mathcal{R}_0^{(1)} > \mathcal{R}_0^{(2)} > 1 \Rightarrow 1 - \frac{1}{\mathcal{R}_0^{(1)}} > 1 - \frac{1}{\mathcal{R}_0^{(2)}} > 0 \Rightarrow \frac{L_{21}}{L_{12}} > \frac{K_2}{K_1} = \frac{(1 - 1/\mathcal{R}_0^{(2)})N_2^*}{(1 - 1/\mathcal{R}_0^{(1)})N_1^*}$$

that line $\overrightarrow{OA}$ is below line $\overrightarrow{OB}$ in $\text{int}\mathbb{R}_+^2$.

(1) $\frac{K_2}{K_1} = \frac{r_1K_2}{r_2K_1} \Leftrightarrow r_1 = r_2 \Leftrightarrow -r_1/r_2 = -1$. The line $\overrightarrow{OA}$ coincides with $\overrightarrow{OC}$ and the tangent line $\mathscr{T}_a$ coincides with $\mathscr{L}_a$. Thus the ellipse $\mathscr{E}_a$ is below $\mathscr{L}_a$ except for the point A, and hence $T_2(\varepsilon) \le T_2(0)$ for $\varepsilon \ge 0$.

(2) $\frac{K_2}{K_1} > \frac{r_1K_2}{r_2K_1} \Leftrightarrow r_1 < r_2 \Leftrightarrow -r_1/r_2 > -1$. The line $\overrightarrow{OB}$ is above line $\overrightarrow{OA}$ and line $\overrightarrow{OA}$ is above line $\overrightarrow{OC}$ in $\text{int}\mathbb{R}_+^2$. Therefore, the arc $\widehat{AB}$ is below the line $\mathscr{L}_a$, and hence $T_2(\varepsilon) \le T_2(0)$ for $\varepsilon \ge 0$.

(3) $\frac{K_2}{K_1} < \frac{r_1K_2}{r_2K_1} \Leftrightarrow r_1 > r_2 \Leftrightarrow -r_1/r_2 < -1$. The line $\overrightarrow{OA}$ is below both lines $\overrightarrow{OB}$ and $\overrightarrow{OC}$ in $\text{int}\mathbb{R}_+^2$.

(i) If $\overrightarrow{OB}$ is above $\overrightarrow{OC}$, i.e.,

$$\frac{L_{21}}{L_{12}} > \frac{r_1K_2}{r_2K_1} \Leftrightarrow \frac{1 - 1/\mathcal{R}_0^{(1)}}{1 - 1/\mathcal{R}_0^{(2)}} = \frac{r_1}{r_2} \cdot \frac{\beta_2}{\beta_1} > \frac{r_1}{r_2} \Leftrightarrow \beta_2 > \beta_1,$$

then there exists $\varepsilon_a > 0$ such that the intersection (I_1^*, I_2^*) of $\mathscr{E}_a$ and $\mathscr{P}_\varepsilon$ moves along $\mathscr{E}_a$ from A to C to B as ε varies from 0 to ε_a to ∞. In other words, if $\beta_2 > \beta_1$, then $T_2(\varepsilon) \ge T_2(0)$ for $\varepsilon \in [0, \varepsilon_a]$ and $T_2(\varepsilon) < T_2(0)$ for $\varepsilon \in (\varepsilon_a, \infty)$. Solving ε from the parabola $\mathscr{P}_\varepsilon$ and substituting point C into the expression gives the critical value

$$\begin{aligned}\varepsilon_a &= \frac{r_1r_2K_1K_2(r_1 - r_2)}{(r_1K_2 + r_2K_1)(r_2K_1L_{21} - r_1K_2L_{12})} \\ &= \frac{\beta_1\beta_2(\beta_1 - \gamma_1 - \beta_2 + \gamma_2)}{(\beta_2 - \beta_1)(L_{21}\beta_1 + L_{12}\beta_2)}.\end{aligned}$$

(ii) If $\overrightarrow{OB}$ is below or coincident with $\overrightarrow{OC}$, i.e., $\beta_2 \le \beta_1$, then B belongs to the arc $\widehat{AC}$, which implies that $T_2(\varepsilon) > T_2(0)$ for $\varepsilon > 0$.

Case (b): $\mathcal{R}_0^{(1)} > \mathcal{R}_0^{(2)} = 1$. The ellipse now takes the form

$$\mathscr{E}_b(I_1, I_2) : r_1\left(1 - \frac{I_1}{K_1}\right)I_1 - \beta_2\frac{I_2^2}{N_2^*} = 0.$$

Clearly, in the first quadrant, $\mathscr{E}_b$ passes through points $O(0,0)$ and $P(K_1, 0)$. As ε varies from 0 to ∞, the intersection of $\mathscr{E}_b$ and the parabola $\mathscr{P}_\varepsilon$ moves along the ellipse from $P(K_1, 0)$ to

$$B = \left(\frac{r_1K_1N_2^*L_{12}^2}{r_1N_2^*L_{12}^2 + \beta_2K_1L_{21}^2}, \frac{r_1K_1N_2^*L_{12}L_{21}}{r_1N_2^*L_{12}^2 + \beta_2K_1L_{21}^2}\right),$$

which is the nontrivial intersection of the ellipse $\mathscr{E}_b$ and $\mathscr{P}_\infty$.

Since $T_2(0) = K_1$, we define $\mathscr{L}_b : I_1 + I_2 = K_1$ to compare $T_2(\varepsilon)$ and $T_2(0)$. Direct calculation finds that the ellipse $\mathscr{E}_b$ and the line $\mathscr{L}_b$ have two intersections:

$$P(K_1, 0) \text{ and } C\left(\frac{\beta_2 K_1^2}{r_1 N_2^* + \beta_2 K_1}, \frac{r_1 K_1 N_2^*}{r_1 N_2^* + \beta_2 K_1}\right).$$

The vertical line $\mathscr{T}_b : I_1 = K_1$ is tangent to the ellipse $\mathscr{E}_b$ at point $P(K_1, 0)$. The slopes of $\overrightarrow{OP}$, $\overrightarrow{OB}$, and $\overrightarrow{OC}$ are

$$0, \quad \frac{L_{21}}{L_{12}}, \quad \text{and} \quad \frac{r_1 N_2^*}{\beta_2 K_1},$$

respectively. The line $\overrightarrow{OP}$ is below both lines $\overrightarrow{OB}$ and $\overrightarrow{OC}$.

(1) $\frac{L_{21}}{L_{12}} > \frac{r_1 N_2^*}{\beta_2 K_1} \Leftrightarrow \beta_1 < \beta_2$. The line $\overrightarrow{OC}$ is below line $\overrightarrow{OB}$ but above line $\overrightarrow{OP}$. Then there exists $\varepsilon_b > 0$ such that the intersection (I_1^*, I_2^*) of $\mathscr{E}_b$ and $\mathscr{P}_\varepsilon$ moves along $\mathscr{E}_b$ from P to C to B as ε varies from 0 to ε_b to ∞. Consequently, if $\beta_2 > \beta_1$, then $T_2(\varepsilon) \geq T_2(0)$ for $\varepsilon \in [0, \varepsilon_b]$ and $T_2(\varepsilon) < T_2(0)$ for $\varepsilon \in (\varepsilon_b, \infty)$. Similarly, solving ε from the parabola $\mathscr{P}_\varepsilon$ and substituting point C into the result gives the critical value

$$\varepsilon_b = \frac{r_1^2 \beta_2 K_1 N_2^*}{(r_1 N_2^* + \beta_2 K_1)(\beta_2 K_1 L_{21} - r_1 N_2^* L_{12})} = \frac{\beta_1 \beta_2 (\beta_1 - \gamma_1)}{(\beta_2 - \beta_1)(L_{21}\beta_1 + L_{12}\beta_2)}.$$

(2) $\frac{L_{21}}{L_{12}} \leq \frac{r_1 N_2^*}{\beta_2 K_1} \Leftrightarrow \beta_1 \geq \beta_2$. The line $\overrightarrow{OC}$ is above line $\overrightarrow{OB}$, and line $\overrightarrow{OB}$ is above line $\overrightarrow{OP}$. Therefore, the arc $\widehat{PB}$ is above line $\mathscr{L}_b$, and hence $T_2(\varepsilon) \geq T_2(0)$ for $\varepsilon \geq 0$.

Case (c): $\mathcal{R}_0^{(1)} > \mathcal{R}_0(\infty) = \frac{L_{12}\beta_1 + L_{21}\beta_2}{L_{12}\gamma_1 + L_{21}\gamma_2} \geq 1 > \mathcal{R}_0^{(2)}$. Denote $r_2 = \gamma_2 - \beta_2 > 0$ and $K_2 = (\gamma_2/\beta_2 - 1)N_2^* > 0$. Then the ellipse can be rewritten as

$$\mathscr{E}_c(I_1, I_2) : r_1\left(1 - \frac{I_1}{K_1}\right) I_1 + r_2\left(-1 - \frac{I_2}{K_2}\right) I_2 = 0.$$

In the first quadrant, $\mathscr{E}_c$ passes through points $O(0, 0)$ and $P(K_1, 0)$. As ε varies from 0 to ∞, the intersection of $\mathscr{E}_c$ and the parabola $\mathscr{P}_\varepsilon$ moves along the ellipse from $P(K_1, 0)$ to

$$B = \left(\frac{K_1 K_2 L_{12}(r_1 L_{12} - r_2 L_{21})}{r_1 K_2 L_{12}^2 + r_2 K_1 L_{21}^2}, \frac{K_1 K_2 L_{21}(r_1 L_{12} - r_2 L_{21})}{r_1 K_2 L_{12}^2 + r_2 K_1 L_{21}^2}\right),$$

which is the nonzero intersection of $\mathscr{E}_c$ and $\mathscr{P}_\infty$. Note that $\mathcal{R}_0(\infty) > 1$ implies $r_1 L_{12} > r_2 L_{21}$, so $B \in \text{int}\mathbb{R}_+^2$.

We still define $\mathscr{L}_c : I_1 + I_2 = K_1$. The ellipse $\mathscr{E}_c$ and the line $\mathscr{L}_c$ have two intersections:

$$P(K_1, 0) \text{ and } C\left(\frac{r_2 K_1 (K_1 + K_2)}{r_1 K_2 + r_2 K_1}, \frac{(r_1 - r_2) K_1 K_2}{r_1 K_2 + r_2 K_1}\right).$$

Point C lies in $\text{int}\mathbb{R}_+^2$ if and only if $r_1 > r_2$. The slope of $\mathscr{T}_c$, the tangent line to the ellipse $\mathscr{E}_c$ at point P, is $-\frac{r_1}{r_2}$. The slopes of $\overrightarrow{OP}$, $\overrightarrow{OB}$, and $\overrightarrow{OC}$ are, respectively,

$$0, \quad \frac{L_{21}}{L_{12}}, \quad \text{and} \quad \frac{(r_1 - r_2) K_2}{r_2 (K_1 + K_2)}.$$

(1) $r_1 \le r_2 \Leftrightarrow -r_1/r_2 \ge -1$. The tangent line $\mathscr{T}_c$ is below or coincides with line $\mathscr{L}_c$ in the first quadrant. Therefore, the arc $\widehat{PB}$ is below line $\mathscr{L}_c$, and hence $T_2(\varepsilon) \le T_2(0)$ for $\varepsilon \ge 0$.

(2) $r_1 > r_2$ and $\frac{L_{21}}{L_{12}} > \frac{(r_1-r_2)K_2}{r_2(K_1+K_2)} \Leftrightarrow \frac{L_{21}}{L_{12}} > \frac{L_{21}\beta_1(\beta_1+\beta_2-\gamma_1-\gamma_2)}{L_{12}\beta_2(\beta_1-\gamma_1)+L_{21}\beta_1(\gamma_2-\beta_2)}$ and $-r_1/r_2 < -1$. The line $\overrightarrow{OB}$ is above line $\overrightarrow{OC}$, and line $\overrightarrow{OC}$ is above line $\overrightarrow{OP}$. There exists $\varepsilon_c > 0$ such that the intersection (I_1^*, I_2^*) of $\mathscr{E}_c$ and $\mathscr{P}_\varepsilon$ moves along $\mathscr{E}_c$ from P to C to B as ε varies from 0 to ε_c to ∞. So we have $T_2(\varepsilon) \ge T_2(0)$ for $\varepsilon \in [0, \varepsilon_c]$ and $T_2(\varepsilon) < T_2(0)$ for $\varepsilon \in (\varepsilon_c, \infty)$. Solving ε from the parabola $\mathscr{P}_\varepsilon$ and substituting point C into the result gives the critical value

$$\begin{aligned}\varepsilon_c &= \frac{r_1 r_2 (r_1 - r_2) K_2 (K_1 + K_2)}{(r_1 K_2 + r_2 K_1)(r_2(K_1 + K_2)L_{21} - (r_1 - r_2)K_2 L_{12})} \\ &= \frac{\beta_1(L_{12}\beta_2(\beta_1 - \gamma_1) + L_{21}\beta_1(\gamma_2 - \beta_2))(\beta_1 + \beta_2 - \gamma_1 - \gamma_2)}{(L_{12}(\beta_1(\gamma_1 + \gamma_2) - \beta_1^2 - \beta_2\gamma_1) + L_{21}\beta_1(\gamma_2 - \beta_2))(L_{21}\beta_1 + L_{12}\beta_2)} > 0.\end{aligned}$$

(3) $\frac{L_{21}}{L_{12}} \le \frac{(r_1-r_2)K_2}{r_2(K_1+K_2)} \Leftrightarrow \frac{L_{21}}{L_{12}} \le \frac{L_{21}\beta_1(\beta_1+\beta_2-\gamma_1-\gamma_2)}{L_{12}\beta_2(\beta_1-\gamma_1)+L_{21}\beta_1(\gamma_2-\beta_2)}$ and $-r_1/r_2 < -1$. The line $\overrightarrow{OB}$ is below line $\overrightarrow{OC}$ but above line $\overrightarrow{OP}$. Therefore, the arc $\widehat{PB}$ is above line $\mathscr{L}_c$, and hence $T_2(\varepsilon) \ge T_2(0)$ for $\varepsilon \ge 0$.

Case (d): $\mathcal{R}_0^{(1)} > 1 > \mathcal{R}_0(\infty) = \frac{L_{12}\beta_1 + L_{21}\beta_2}{L_{12}\gamma_1 + L_{21}\gamma_2} > \mathcal{R}_0^{(2)}$. It follows from Remark 3.2 that there exists a unique positive ε^* such that $\mathcal{R}_0(\varepsilon) > 1$ for $\varepsilon \in [0, \varepsilon^*)$ and $\mathcal{R}_0(\varepsilon) < 1$ for $\varepsilon \in (\varepsilon^*, \infty)$. Hence, $T_2(\varepsilon) > 0$ for $\varepsilon \in [0, \varepsilon^*)$ and $T_2(\varepsilon) = 0$ for $\varepsilon \in [\varepsilon^*, \infty)$. Thus, it suffices to consider ε on the interval $[0, \varepsilon^*]$. We define $\mathscr{E}_c$, $\mathscr{L}_c$, $\mathscr{T}_c$, ε_c, and C as in Case (c). As ε varies from 0 to ε^*, the intersection of $\mathscr{E}_c$ and the parabola $\mathscr{P}_\varepsilon$ moves along the ellipse from $P(K_1, 0)$ to $O(0, 0)$. The slopes of $\overrightarrow{OP}$ and $\overrightarrow{OC}$ are, respectively,

$$0 \quad \text{and} \quad \frac{(r_1 - r_2)K_2}{r_2(K_1 + K_2)}.$$

(1) $r_1 \le r_2 \Leftrightarrow -r_1/r_2 \ge -1$. The tangent line $\mathscr{T}_c$ is below or coincides with line $\mathscr{L}_c$. Therefore, the arc $\widehat{PO}$ is below line $\mathscr{L}_c$, and hence $T_2(\varepsilon) \le T_2(0)$ for $\varepsilon \in [0, \varepsilon^*]$.

(2) $r_1 > r_2 \Leftrightarrow -r_1/r_2 < -1$. The line $\overrightarrow{OP}$ is below line $\overrightarrow{OC}$. Therefore, for the same ε_c as in Case (c), the intersection (I_1^*, I_2^*) of $\mathscr{E}_c$ and $\mathscr{P}_\varepsilon$ moves along $\mathscr{E}_c$ from P to C to O as ε varies from 0 to ε_c to ε^*. Hence we have $T_2(\varepsilon) \ge T_2(0)$ for $\varepsilon \in [0, \varepsilon_c]$ and $T_2(\varepsilon) < T_2(0)$ for $\varepsilon \in (\varepsilon_c, \varepsilon^*]$.

Case (e): $1 \ge \mathcal{R}_0^{(1)} > \mathcal{R}_0^{(2)}$. Since $\mathcal{R}_0(\varepsilon) < 1$ for $\varepsilon > 0$, the disease-free equilibrium E_0 is globally asymptotically stable, which means that $T_2(\varepsilon) \equiv 0$ for $\varepsilon \ge 0$. ∎

Remark. Suppose that $\mathcal{R}_0^{(1)} > \mathcal{R}_0^{(2)}$. Theorem 4.3 indicates that if $0 < \beta_1 - \gamma_1 \le |\beta_2 - \gamma_2|$, i.e., $0 < r_1 \le r_2$, then $T_2(\varepsilon) < T_2(0)$ for $\varepsilon > 0$. This can be easily proved in a unified way. In fact, the condition $0 < r_1 \le r_2$ implies $-r_1/r_2 \ge -1$, so $\mathscr{T}_a$ (or $\mathscr{T}_c$), the tangent line of the ellipse $\mathscr{E}_a$ (or $\mathscr{E}_c$) at A (or P), is below or coincides with line $\mathscr{L}_a$ (or $\mathscr{L}_c$). As ε varies from 0 to ∞ (or ε^*), the intersection of the ellipse and the parabola moves counterclockwise on the ellipse from A (or P) to B (or O). Thus, the arc $\widehat{AB}$ (or $\widehat{PB}$ or $\widehat{PO}$) is wholly below line $\mathscr{L}_a$ (or $\mathscr{L}_c$), and hence $T_2(\varepsilon) < T_2(0)$ for $\varepsilon > 0$.

Acknowledgments. The author is grateful to the two anonymous reviewers for their valuable comments, and Drs. Yijun Lou and Shigui Ruan for helpful discussions.

REFERENCES

[1] L. J. S. Allen, B. M. Bolker, Y. Lou, and A. L. Nevai, *Asymptotic profiles of the steady states for an SIS epidemic patch model*, SIAM J. Appl. Math., 67 (2007), pp. 1283–1309, https://doi.org/10.1137/060672522.

[2] L. J. S. Allen, B. M. Bolker, Y. Lou, and A. L. Nevai, *Asymptotic profiles of the steady states for an SIS epidemic reaction-diffusion model*, Discrete Contin. Dyn. Syst. Ser. A, 21 (2008), pp. 1–20.

[3] R. Arditi, C. Lobry, and T. Sari, *Is dispersal always beneficial to carrying capacity? New insights from the multi-patch logistic equation*, Theor. Popul. Biol., 106 (2015), pp. 45–59.

[4] R. Arditi, C. Lobry, and T. Sari, *Asymmetric dispersal in the multi-patch logistic equation*, Theor. Popul. Biol., 120 (2018), pp. 11–15.

[5] J. Arino, *Diseases in metapopulations*, in Modeling and Dynamics of Infectious Diseases, Z. Ma, Y. Zhou, and J. Wu, eds., Ser. Contemp. Appl. Math., World Scientific, Singapore, 2009, pp. 64–122.

[6] J. Arino and S. Portet, *Epidemiological implications of mobility between a large urban centre and smaller satellite cities*, J. Math. Biol., 71 (2015), pp. 1243–1265.

[7] C. Castillo-Chavez and H. Thieme, *Asymptotically autonomous epidemic models*, in Mathematical Population Dynamics: Analysis of Heterogeneity, Vol. 1, Theory of Epidemics, O. Arino, D. Axelrod, M. Kimmel, and M. Langlais, eds., Wuerz, Winnipeg, 1995, pp. 33–50.

[8] S. Chen, J. Shi, Z. Shuai, and Y. Wu, *Asymptotic profiles of the steady states for an SIS epidemic patch model with asymmetric connectivity matrix*, J. Math. Biol., 80 (2020), pp. 2327–2361.

[9] C. Cosner, J. C. Beier, R. S. Cantrell, D. Impoinvil, L. Kapitanski, M. D. Potts, A. Troyo, and S. Ruan, *The effects of human movement on the persistence of vector-borne diseases*, J. Theor. Biol., 258 (2009), pp. 550–560.

[10] J. Cui, Y. Takeuchi, and Y. Saito, *Spreading disease with transport-related infection*, J. Theor. Biol., 239 (2006), pp. 376–390.

[11] D. L. DeAngelis, W.-M. Ni, and B. Zhang, *Effects of diffusion on total biomass in heterogeneous continuous and discrete-patch systems*, Theor. Ecol., 9 (2016), pp. 443–453.

[12] O. Diekmann, J. A. P. Heesterbeek, and J. A. Metz, *On the definition and the computation of the basic reproduction ratio R_0 in models for infectious diseases in heterogeneous populations*, J. Math. Biol., 28 (1990), pp. 365–382.

[13] C. Dye and G. Hasibeder, *Population dynamics of mosquito-borne disease: Effects of flies which bite some people more frequently than others*, Trans. R. Soc. Trop. Med. Hyg., 80 (1986), pp. 69–77.

[14] H. I. Freedman, B. Rai, and P. Waltman, *Mathematical models of population interactions with dispersal.* II: *Differential survival in a change of habitat*, J. Math. Anal. Appl., 115 (1986), pp. 140–154.

[15] H. I. Freedman and P. Waltman, *Mathematical models of population interactions with dispersal.* I: *Stability of two habitats with and without a predator*, SIAM J. Appl. Math., 32 (1977), pp. 631–648, https://doi.org/10.1137/0132052.

[16] S. D. Fretwell and H. L. Lucas, *On territorial behavior and other factors influencing habitat distribution in birds.* I: *Theoretical development*, Acta Biotheor., 19 (1969), pp. 16–36.

[17] D. Gao, *Travel frequency and infectious diseases*, SIAM J. Appl. Math., 79 (2019), pp. 1581–1606, https://doi.org/10.1137/18M1211957.

[18] D. Gao and C.-P. Dong, *Fast diffusion inhibits disease outbreaks*, Proc. Amer. Math. Soc., 148 (2020), pp. 1709–1722.

[19] D. Gao and Y. Lou, *Impact of state-dependent dispersal on disease prevalence*, under review, 2020.

[20] D. Gao and S. Ruan, *An SIS patch model with variable transmission coefficients*, Math. Biosci., 232 (2011), pp. 110–115.

[21] D. Gao and S. Ruan, *A multipatch malaria model with logistic growth populations*, SIAM J. Appl. Math., 72 (2012), pp. 819–841, https://doi.org/10.1137/110850761.

[22] D. Gao, P. van den Driessche, and C. Cosner, *Habitat fragmentation promotes malaria persistence*, J. Math. Biol., 79 (2019), pp. 2255–2280.

[23] G. Hasibeder and C. Dye, *Population dynamics of mosquito-borne disease: Persistence in a completely heterogeneous environment*, Theor. Popul. Biol., 33 (1988), pp. 31–53.

[24] R. D. Holt, *Population dynamics in two-patch environments: Some anomalous consequences of an optimal habitat distribution*, Theor. Popul. Biol., 28 (1985), pp. 181–208.

[25] Y.-H. Hsieh, P. van den Driessche, and L. Wang, *Impact of travel between patches for*

spatial spread of disease, Bull. Math. Biol., 69 (2007), pp. 1355–1375.
[26] Y. Jin and W. Wang, *The effect of population dispersal on the spread of a disease*, J. Math. Anal. Appl., 308 (2005), pp. 343–364.
[27] K. Khan, J. Arino, W. Hu, P. Raposo, J. Sears, F. Calderon, C. Heidebrecht, M. Macdonald, J. Liauw, A. Chan, and M. Gardam, *Spread of a novel influenza A (H1N1) virus via global airline transportation*, New Eng. J. Med., 361 (2009), pp. 212–214.
[28] H. Li and R. Peng, *Dynamics and asymptotic profiles of endemic equilibrium for SIS epidemic patch models*, J. Math. Biol., 79 (2019), pp. 1279–1317.
[29] M. Y. Li and Z. Shuai, *Global stability of an epidemic model in a patchy environment*, Can. Appl. Math. Q., 17 (2009), pp. 175–187.
[30] X. Liu and Y. Takeuchi, *Spread of disease with transport-related infection and entry screening*, J. Theor. Biol., 242 (2006), pp. 517–528.
[31] Y. Lou, *On the effects of migration and spatial heterogeneity on single and multiple species*, J. Differential Equations, 223 (2006), pp. 400–426.
[32] K. E. Mace, P. M. Arguin, N. W. Lucchi, and K. R. Tan, *Malaria Surveillance - United States,* 2016, MMWR Morb. Mortal. Wkly. Rep. Surveillance Summaries, 68 (2019), pp. 1–35.
[33] S. Ruan, W. Wang, and S. A. Levin, *The effect of global travel on the spread of SARS*, Math. Biosci. Eng., 3 (2006), pp. 205–218.
[34] M. Salmani and P. van den Driessche, *A model for disease transmission in a patchy environment*, Discrete Contin. Dyn. Syst. Ser. B, 6 (2006), pp. 185–202.
[35] H. L. Smith, *Monotone Dynamical Systems: An Introduction to the Theory of Competitive and Cooperative Systems*, Math. Surveys Monogr. 41, AMS, Providence, RI, 1995.
[36] C. Sun, W. Yang, J. Arino, and K. Khan, *Effect of media-induced social distancing on disease transmission in a two patch setting*, Math. Biosci., 230 (2011), pp. 87–95.
[37] Y. Takeuchi, *Cooperative systems theory and global stability of diffusion models*, in Evolution and Control in Biological Systems, A. B. Kurzhanski and K. Sigmund, eds., Springer, Dordrecht, 1989, pp. 49–57.
[38] R. B. Turner, *The epidemiology, pathogenesis, and treatment of the common cold*, Semin. Pediatr. Infect. Dis., 6 (1995), pp. 57–61.
[39] P. van den Driessche and J. Watmough, *Reproduction numbers and sub-threshold endemic equilibria for compartmental models of disease transmission*, Math. Biosci., 180 (2002), pp. 29–48.
[40] W. Wang, *Population dispersal and disease spread*, Discrete Contin. Dyn. Syst. Ser. B, 4 (2004), pp. 797–804.
[41] W. Wang, *Epidemic models with population dispersal*, in Mathematics for Life Science and Medicine, Y. Takeuchi, Y. Iwasa, and K. Sato, eds., Springer, Berlin, 2007, pp. 67–95.
[42] W. Wang and G. Mulone, *Threshold of disease transmission in a patch environment*, J. Math. Anal. Appl., 285 (2003), pp. 321–335.
[43] W. Wang and X.-Q. Zhao, *An epidemic model in a patchy environment*, Math. Biosci., 190 (2004), pp. 97–112.
[44] Y. Wang, *Pollination-mutualisms in a two-patch system with dispersal*, J. Theor. Biol., 476 (2019), pp. 51–61.
[45] World Health Organization, *Zika Situation Report - 28 July* 2016, 2016, https://www.who.int/emergencies/zika-virus/situation-report/28-july-2016/en/.
[46] World Health Organization, *Coronavirus Disease (COVID-2019) Situation Reports*, 2020, https://www.who.int/emergencies/diseases/novel-coronavirus-2019/situation-reports.
[47] B. Zhang, A. Kula, K. M. L. Mack, L. Zhai, A. L. Ryce, W.-M. Ni, D. L. DeAngelis, and J. D. Van Dyken, *Carrying capacity in a heterogeneous environment with habitat connectivity*, Ecol. Lett., 20 (2017), pp. 1118–1128.